MNRAS **000**, 1–18 (2011) Preprint 17 June 2021 Compiled using MNRAS LATEX style file v3.0

Rapidly-oscillating *TESS* A–F main sequence stars

L. A. Balona
South African Astronomical Observatory, P.O. Box 9, Observatory, Cape Town, South Africa

Accepted .... Received ...

ABSTRACT

From sector 1–36 *TESS* observations, 18 new roAp stars, 82 ostensibly non-peculiar stars with roAp-like frequencies (the "roA" variables) and 88 δ Scuti stars with independent frequencies typical of roAp stars were found. There is no criterion that can distinguish roAp/roA stars from δ Sct stars, but for expediency an arbitrary low frequency limit of $60\,\mathrm{d}^{-1}$ was chosen. Because an unknown mode selection process is clearly present in δ Sct stars, the roAp/roA stars may be considered as δ Sct stars in which high frequencies are preferentially selected. This interpretation is supported by the fact that the combined proportion of δ Sct and roAp stars among Ap stars is the same as among non-Ap stars. Contrary to models, observations show that low frequencies in Ap stars are not strongly suppressed. One of the most puzzling aspects of roAp stars is the large fraction which have short mode lifetimes. The failure of current models to explain these results may be due to an incorrect treatment of the outer layers of these stars.

Key words: stars:oscillations; stars: chemically peculiar

1 INTRODUCTION

The peculiar Ap and Fp stars have strong, approximately dipolar, kilogauss global magnetic fields with axes which are generally tilted with respect to the rotation axes. They have inhomogeneous surface abundances and brightness, leading to rotational light modulation (the oblique rotator model Stibbs 1950). Their spectra have unusually strong lines of some ionized metals (e.g., Sr, Cr) and rare earth elements. The chemical peculiarities, which are confined to the outer layers, are thought to be a result of radiative acceleration, gravitational settling and diffusion.

The rapidly-oscillating Ap (roAp) stars are Ap/Fp stars which pulsate in a limited high-frequency range, typically above $60\,\mathrm{d}^{-1}$ (Kurtz 1978, 1982). Such high frequencies are not predicted in standard models in which the opacity κ mechanism drives pulsations. However, driving of high-frequency oscillations similar to those observed in roAp stars is possible if a temperature inversion is present in the lower atmosphere (Gautschy et al. 1998). The temperature inversion, which need only be 1000–3000 K, raises the superficial critical frequency sufficiently to reflect the high-frequency modes. Recent models by Xiong et al. (2016) do, however, predict roAp-like frequencies in standard models, but only in a restricted region of the H–R diagram.

In conventional models, pulsational driving due to the κ mechanism acting in the H/He I partial ionization zone is almost enough to overcome damping in the rest of the star. This led Balmforth et al. (2001) to suggest that suppression of convection by a vertical magnetic field might be sufficient to reduce damping, resulting in driving of high-frequency pulsations confined to the region around the magnetic poles (see also Cunha 2002, Cunha et al. 2013). More recent models, which include time-dependent convection, show that even non-magnetic normal A stars of about $2\,M_\odot$ are unstable with frequencies as high as $200\,\mathrm{d}^{-1}$ (Xiong et al. 2016).

The δ Scuti/γ Doradus pulsational variables are free from the effect of the strong global magnetic field and inhomogeneous surface abundances and are easier to model. In spite of this, current models are unable to reproduce the low frequencies (i.e. below $5\,\mathrm{d}^{-1}$) which are ubiquitous in δ Sct stars (Balona 2014). Current models also cannot explain why pulsation mode selection varies so widely among stars with approximately the same physical parameters (Balona et al. 2015). Neither can they reproduce the fact that both γ Dor and δ Sct stars co-exist in the same effective temperature and luminosity region (Balona 2018a). Another problem is that less than half of the stars in the δ Sct instability region seem to pulsate(Balona 2018a). Furthermore, current models have no explanation for high frequencies (typically higher than $5\,\mathrm{d}^{-1}$ seen in mid- to late-B main sequence stars (the Maia variables, Balona & Ozuyar 2020).

Until we understand and can model these much simpler stars, it is difficult to see how progress in understanding the roAp stars can be achieved. Perhaps a large part of the problem is the realization that current ideas regarding the upper layers of radiative atmospheres may need to be revised. Observations of thousands of stars from the *Kepler* and *TESS* missions clearly show that rotational light modulation is present in a large fraction of normal (i.e. non-

peculiar) upper main-sequence stars (Balona 2019, 2021), presumably a result of starspots. Starspots require a local magnetic field. Magnetic fields in stars are thought to be generated by dynamo action in convective regions. It is possible that convective or turbulent motions are present in the upper layers of A and B stars, even though they have long been regarded as having static photospheres in radiative equilibrium.

It is clear that we cannot be guided by current pulsational models in understanding the roAp stars. The best approach is to obtain further observations which might provide clues on their nature. For this purpose, the *TESS* data is of great importance. The search for new roAp or roAp-like stars in the first few months of this mission has been reported by Cunha et al. (2019) and Balona et al. (2019). Some results from these initial studies are quite surprising. There is the issue of whether or not roAp-like pulsations are confined to chemically peculiar stars with strong global magnetic fields or whether such high frequencies may exist in apparently non-peculiar stars. In a more recent study, Holdsworth et al. (2021) find that many of the non-peculiar stars are indeed Ap stars, but it is still not possible to rule out this possibility completely. The question of what criteria are used to classify a star as roAp is still uncertain. In this paper we present new detections of high frequency pulsations in *TESS* A and F stars from sectors 1–36 stars and discuss results which may have a bearing on the nature of these stars.

2 THE DATA AND VARIABILITY CLASSIFICATION

The *TESS* photometric survey consists of continuous wide-band photometry of 13 sectors per celestial hemisphere. Each sector is observed continuously for about 27 days with 2-min cadence. Stars near the ecliptic equator are only observed for one sector. Stars in the circular regions nearer the poles overlap so that, at the ecliptic poles, stars are observed continuously for about 100 days. The data used here are from sectors 1–36 which covers the whole sky with some overlap. The light curves are corrected for time-correlated instrumental signatures using pre-search data conditioning (PDC, Jenkins et al. 2016). All available *TESS* data up to and including sector 36 are used for each star in this paper.

The most important step in any survey of this nature is to determine the variability type of each star. There is little doubt that at some time in the future such a task will be possible using computational means. At present, however, automation has not produced satisfactory results whenever it has been attempted. For this reason, visual inspection of the data (light curves and periodograms) seems to be the only satisfactory option.

A catalogue of variability type in over 95 000 stars hotter than about 6000 K observed by *TESS* and *Kepler*, has been compiled by visual inspection of their periodograms and light curves. This catalogue began with a list of about 684000 stars brighter than magnitude 12.5 and with spectral types earlier than G0. The spectral types are important as it offers clues as to the type of variability of a star. As each *TESS* sector is released, stars in the bulk download file are matched with this catalogue and downloaded. The light curve from the FITS file is extracted automatically and stored in a database. If the star is already in the database, the additional data is appended to the existing light curve. Periodograms are automatically calculated for all stars that have been downloaded. Frequency extraction is also automated. The periodograms and frequency lists also form part of the database. Usually there are about 1000–2000 new stars that require classification after each *TESS* release. Tools are available to display the periodogram, extracted frequencies and light curve of each star with a click of a button. The software interface also contains tools for smoothing the light curve, identifying harmonics and other useful functions. The task of visually classifying 1000–2000 stars typically takes two days. Changes are sometimes made to previously classified stars as more data becomes available.

The variability classification follows that of the *General Catalogue of Variable Stars* (GCVS, Samus et al. 2017). Rotational light modulation due to chemical abundance spots in A stars are classified as the α^2 CVn (ACV) variables. Among the B stars these are known as SX Ari (SXARI) variables. A new ROT class has been added to describe any star, not known to be chemically peculiar, in which the variability is suspected to be due to rotation. A rough estimate of the spectral type or effective temperature, $T_{\rm eff}$, is necessary in order to distinguish β Cep, SPB and Maia stars from δ Sct, γ Dor and roAp variables.

For each star, the literature was searched for estimates of the effective temperature, $T_{\rm eff}$, projected rotational velocity, $v \sin i$, and spectral type. Photometric effective temperatures for Ap stars are unreliable because of line blanketing due to the spectral peculiarities. A catalogue of over 101500 stars comprising about 185000 individual $T_{\rm eff}$ measurements using various methods was compiled. These are over and above the effective temperatures from the *Kepler* and *TESS* catalogues. An algorithm was used to select the most appropriate value value of $T_{\rm eff}$ for each star. Whenever possible, values of $T_{\rm eff}$ derived from spectroscopic modelling are selected. Spectral types are mostly from the catalogue of Skiff (2014) supplemented by later publications when required.

The stellar luminosity was estimated from *Gaia* DR2 parallaxes (Gaia Collaboration et al. 2016, 2018) in conjunction with reddening obtained from a three-dimensional map by Gontcharov (2017) using the bolometric correction calibration by Pecaut & Mamajek (2013). From the error in the *Gaia* DR2 parallax, the typical standard deviation in $\log(L/L_\odot)$ is estimated to be about 0.05 dex, allowing for standard deviations of 0.01 mag in the apparent magnitude, 0.10 mag in visual extinction and 0.02 mag in the bolometric correction in addition to the parallax error.

A catalogue of projected rotational velocities, $v \sin i$, consisting of over 58000 individual measurements of 35200 stars was compiled. The bulk of these measurements are from Głębocki & Gnaciński (2005). The catalogue was brought up to date by a literature search.

3 A CLASSIFICATION PROBLEM

For a classification scheme to be useful, each class needs to be well defined. Unfortunately, the characteristics that define a roAp star are not at all clear. The general view is that roAp stars are simply Ap stars with high frequencies, but there is no consensus on the meaning of "high fre-

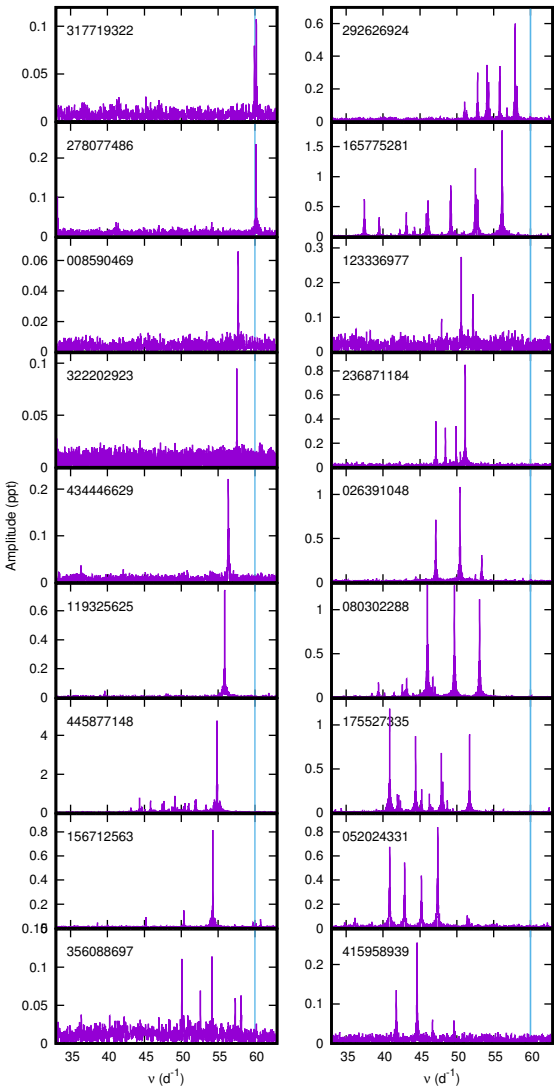

Figure 1. Stars with a dominant high peak at high frequencies. The vertical line is the frequency above which these stars would be classified as ROAP. The TIC numbers are shown. All stars are non-peculiar except for TIC 39818458 which is an Ap star.

quencies". The lowest frequency in the group of recognized roAp stars (as listed in Smalley et al. 2015) is $61\,\mathrm{d}^{-1}$, but recently Holdsworth et al. (2021) admitted TIC 356088697, which has a single pulsation mode at $55.8\,\mathrm{d}^{-1}$, to the list of roAp stars. What is the status of Ap stars with peaks in the δ Sct range as well as in the the roAp range? One solution is to classify these as DSCT+ROAP. But then there are Ap stars where all the peaks are in the narrow range $50 < \nu < 60\,\mathrm{d}^{-1}$ as in TIC 39818458 (Fig. 1). Is this just DSCT or should one shift the criterion down to $50\,\mathrm{d}^{-1}$ and classify the star as ROAP? If we shift the criterion to $50\,\mathrm{d}^{-1}$, then how do we classify TIC 194356599, an Ap star with two strong peaks at 46.7 and $50.4\,\mathrm{d}^{-1}$ and weaker peak at $61.1\,\mathrm{d}^{-1}$? Do we now move the criterion to, say, $45\,\mathrm{d}^{-1}$, which then opens up further stars which meet the new definition for ROAP.

This problem is not new (Balona et al. 2019; Khalack et al. 2019). It arises because we do not have

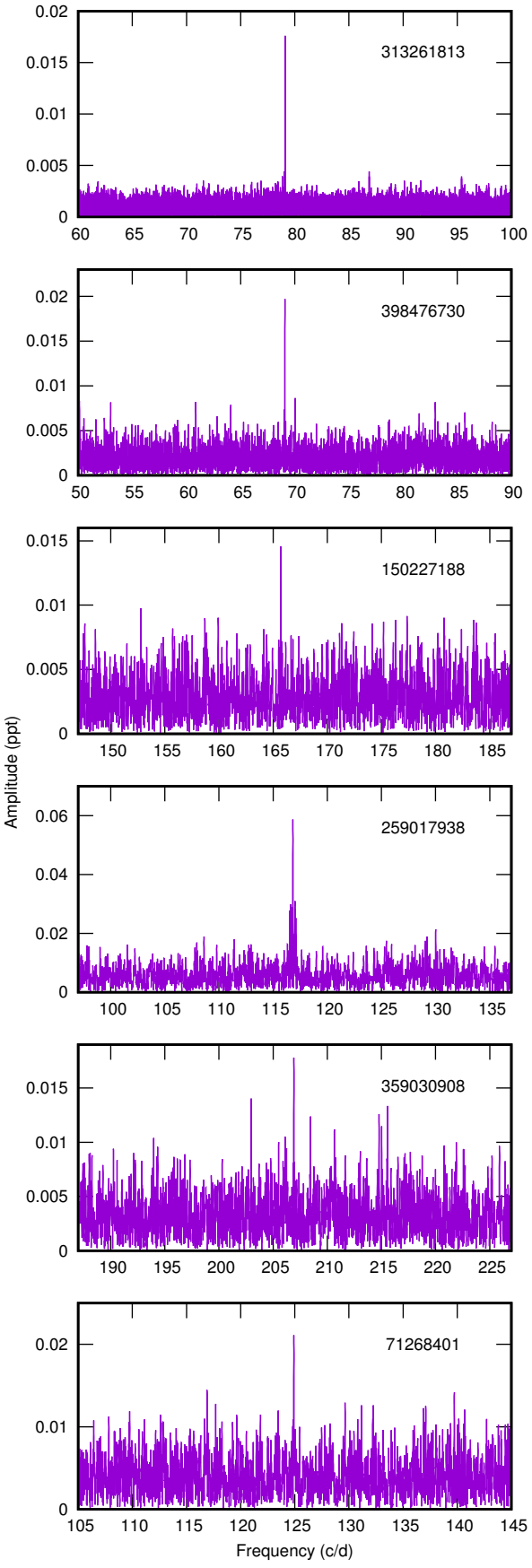

Figure 2. Examples of bright stars, not known to be chemically peculiar, with high roAp-like frequencies.

a working model for roAp stars nor for δ Sct stars. We do not know what to look for as theory is unable to provide a guide. As mentioned in the introduction, standard models of these stars fail to reproduce the high frequencies unless convection is suppressed at the poles. However, the models with suppressed convection fail to reproduce the instability strip of the roAp stars (Cunha 2002). Furthermore, they predict that low frequencies should be strongly damped Murphy et al. (2020), which is not the case for Ap stars which are δ Sct pulsators (see below). We now know that δ Sct pulsations are fairly common among Ap stars (see below). If this fact was known when roAp stars were first discovered, they might have been classified as just δ Sct stars with particularly high frequencies.

Another problem is how to classify stars which have frequencies typical of roAp stars, but are not known to be chemically peculiar. It is, of course, possible that all these stars have been mis-classified. Indeed, Holdsworth et al. (2021) obtained spectra and showed that many stars classified as chemically normal are Ap stars. It has been known for many years that there are chemically normal δ Sct stars with independent frequencies in the roAp range (example Balona et al. 2012). There is certainly no compelling reason to assume that all stars with roAp-like frequencies are chemically peculiar. Indeed, it would be incorrect to make such an assumption, especially since the most recent models predict high-frequency oscillations in models of chemically normal massive A stars (Xiong et al. 2016). However, the models are stable for less massive stars which include most of the δ Sct stars in the instability strip having roAp-like frequencies. For this reason, apparently chemically normal stars with unexplained roAp-like frequencies will be called "roA" stars until they are shown to be chemically peculiar or until the driving mechanism has been understood.

The classification problem for roAp stars applies to roA stars as well. In this paper, a star is classified as roAp or roA only if at least one frequency peak higher than $60\,\mathrm{d}^{-1}$ is present. As an illustration of why the arbitrary choice of $60\,\mathrm{d}^{-1}$ (or any other frequency) is so unsatisfactory is given in Fig. 1. In the left panel we show the periodograms of stars with just a single dominant high frequency and no other feature apart from, in a few cases, the rotational peaks. There are many established roAp stars with just a single frequency above $60\,\mathrm{d}^{-1}$, but, as can be seen in the figure, there are equally quite a number of stars, both Ap and non-Ap, with peaks at slightly lower frequencies as discussed above. There are other examples cited above. The limit of $60\,\mathrm{d}^{-1}$ is merely a convenience dictated by the history of discovery.

Some roAp stars are characterised by nearly equally-spaced peaks which are attributed to a sequence of modes of the same spherical harmonic, but of sequential radial order, n. Here again, one can find many stars with very similar sequential peaks near the artificial 60^{-1} frequency boundary, as shown in the right hand panels of Fig. 1. These stars are examples of the high-frequency δ Sct stars discussed in Bedding et al. (2020) in which a pattern of around four strong peaks in the range 40–$50\,\mathrm{d}^{-1}$ is quite common.

Given sufficient precision, pulsation modes with frequencies typical of δ Sct or γ Dor stars are often detected in roAp stars. An example is the case of the roAp star KIC 11296437 (Murphy et al. 2020). In the *TESS* data only the high-frequency peak at $121.8\,\mathrm{d}^{-1}$ is visible, but the *Kepler* data, which have higher precision, shows additional peaks at around $10\,\mathrm{d}^{-1}$. In this case the separation between the δ Sct and roAp peaks is very large and there is merit in calling it a δ Sct+roAp hybrid. However, there are many δ Sct stars with independent peaks extending well into the roAp region. These are chemically normal stars, but yet they satisfy the frequency criterion for roA stars. Because there is no clear frequency break between the δ Sct and roA frequencies, there is less on an inclination to classify these as δ Sct+roA hybrids. However, this would be inconsistent with the above definition and in this paper we classify these stars as DSCT+ROA. The ROA classification on its own is reserved for stars with no peaks below $60\,\mathrm{d}^{-1}$.

Table 1 lists all known roAp/roA stars, even those not observed by *TESS*. This is essentially the list in Smalley et al. (2015) supplemented by *TESS* discoveries by Cunha et al. (2019) and Balona et al. (2019) and, most recently, by Holdsworth et al. (2021).

It should be noted that there are 9 stars known to be roAp from ground-based observations, but which do not have any significant high frequencies in the *TESS* data. In the tables, these are represented by the classification [ROAP]. In two of them, TIC 27395746 and TIC 158216369, the roAp identification is a result of extending the frequencies beyond the Nyquist limit (Hey et al. 2019). Because the *Kepler* have higher S/N than *TESS*, the high frequencies are not detected in *TESS* observations of TIC 169078762 (Smalley et al. 2015) and TIC 272598185 (Balona et al. 2011a).

The others are from radial velocity detections: TIC 35905913 (Kochukhov et al. 2013), TIC 173372645 (Kurtz et al. 2006a), TIC 93522454 (Elkin et al. 2010; Kochukhov et al. 2013) and TIC 125297016 and TIC 168383678 (Elkin et al. 2010; Kochukhov et al. 2013). High-precision radial velocities are better at detecting roAp stars than photometry. One needs to bear in mind that *TESS* is not the optimal instrument for a survey of roAp oscillations and that many roA and roAp undoubtedly remain undetected.

Table 2 lists previously unreported *TESS* stars with effective temperatures $T_{\rm eff} > 6000\,\mathrm{K}$ in which at least one significant, independent frequency peak higher than $60\,\mathrm{d}^{-1}$ is present. The test for significance is based on the commonly used criterion that the peak amplitude must exceed the mean local noise level by a factor of four. This significance criterion is discussed in Koen (2010). The test for independent high frequencies in δ Sct stars will be described below.

There are a large number of stars in Table 2 which are not known to be chemically peculiar. It would be expected that spectral classification of bright stars should have detected the chemical peculiarities characteristic of Ap stars. Table 2 contains at least a dozen stars brighter than 8-th magnitude. Six of these are listed in Table 3 and their periodograms shown in Fig. 2. As can be seen, these would certainly be classified as roAp stars even though they are supposedly non-peculiar. HD 119476 (TIC 313261813), for example, has been classified in the range B9V–A2V by seven different authors (Skiff 2014).

Fig 3 shows the location of all roAp and roA stars in the theoretical H–R diagram. Also included are the empir-

Table 1. List of known roAp stars. The TIC number, name, variability type and characteristic pulsation frequency is given, followed by the effective temperature and luminosity. Where available, the rotation period is given. The last column is the spectral type. A colon denotes uncertain values. The variability class is expanded to include the following: r - rotational sidelobes present; s - variable amplitudes and/or frequencies; 2h,3h - highest harmonic present; l - low frequencies present. A row in italics indicates that the star was not observed by *TESS*. The variability type in square brackets means that the high frequencies are not detected in the *TESS* light curve

TIC	Name	Var Type	ν (d^{-1})	$T_{\rm eff}$ (K)	$\log \frac{L}{L_\odot}$ (dex)	$P_{\rm rot}$ (d)	Sp Type
3814749	HD 3748	ROT+ROA	238.205	7945	1.12	1.689	A5
6118924	HD 116114	ROAP	66.461	8013	1.43		F0VpSrCrEu
12968953	HD 217704	ROAP	115.586	7972	1.42		ApSrEuCr*
16596302	HD 52524	ROT+ROA:	74.156	8733	0.98	2.532	A0
17676722	HD 63773	ACV+ROAP+r	167.749	8754	1.26	1.599	ApSrEuCr*
22113439	TYC 2612-1843-1	ACV+ROAP	62.639	8112	1.38	2.119	A7m:
22132451	*2MASS J17584421+3458339*	*DSCT/ROAP*	*71.280*	*8150*	*1.12*		*A7m:*
23671771	HD 70664	ROT+ROA	293.202	6223	0.89	6.135	F5
24344701	HD 34282	ROA	75.412	9500	1.15		A0.5Vb(shell)
26418690	KIC 11296437	DSCT+ROAP+r	121.800	7450	1.18		Ap
26749633	*TYC 3560-2018-1*	*ROAP*	*118.603*	*7000*	*1.18*		*F2V(Sr)*
27395746	KIC 11409673	ACV+[ROAP]+r	216.080	7500	1.06	12.214	Ap
33601621	HD 42659	ACV+ROAP+r	150.990	7698	1.55	2.659	A3SrCrEu
34783979	TYC 1787-186-1	ROA:	233.958	6047	0.12		
35905913	HD 132205	ACV+[ROAP]	201.658	9400	1.15	7.535	A2EuSrCr
41259805	HD 43226	ACV+ROAP+r	199.673	8721	1.27	1.714	ApSrEu(Cr)*
44827786	HD 150562	ROAP	133.661	6726	1.07		A5:EuSi??
49332521	HD 119027	ROAP	167.790	6886	1.11		ApSrEuCr:
49818005	HD 19687	ROAP	141.860	7214	0.89		FpSrEu(Cr)*
58106971	*TYC 2269-996-1*	*DSCT+ROA*	*79.130*	*6650*	*1.02*		*A0V*
61811148	TYC 7926-99-1	DSCT+ACV+ROAP	164.475	6639	0.83	0.848	A7m
69855370	HD 213637	ROAP	125.479	6587	0.78		Ap:Eu:Sr:Cr:
71134596	HD 28548	DSCT+ROA	65.245	8200	1.09		A0IV/V λ Boo
72428505	*HD 195061*	*DSCT+ROAP*	*128.860*	*9900*	*1.06*		*A0Vm*
77128654	HD 97127	ROAP+r	106.618	6407	0.95		F3pSrEu(Cr)
92350273	CD-33 15279	ROT+ROA	244.814	6389	1.53	6.622	F5
93522454	HD 143487	[ROAP]	149.472	8731	1.49		A3SrEuCr?
96315731	HD 51203	ACV+ROAP	165.259	7694	1.07	6.674	ApSrEuCr
96855460	HD 185256	ACV:+ROAP	140.628	7100	1.04	26.329	ApSrEu:Cr:
98728812	HD 18407	ROA	65.301	9159	1.34		A0V
100196783	*HD 193756*	*ROAP*	*111.024*	*7650*	*1.44*		*A9SrCrEu*
100775380	HD 39763	GDOR+ROA	68.860	8420	1.4:		A1V
118247716	HD 12519	ROAP	170.288	7403	0.98		A4pSrEuCr
119327278	HD 45698	ACV+ROAP+r	210.614	8445	1.22	1.085	A2SrEu
123231021	KIC 7582608	GDOR+ACV:+ROAP	181.699	8148	1.41	9.906	A7pEuCr
125297016	HD 69013	[ROAP]	128.304	6951	1.11		A2SrEu
128821559	*TYC 3218-888-2*	*DSCT/ROAP*	*75.540*	*9150*	*1.10*		*A3m*
136842396	HD 9289	ACV+ROAP+r	136.953	7900	0.87	8.566	A3SrEuCr
137797293	TYC 6390-339-1	DSCT/ROA	66.960	9150	1.09		A3
138093523	TYC 3139-1403-1	DSCT+ROA	129.030	7360	0.97		
139191168	HD 217522	ROAP+s	104.179	6918	0.95		A5SrEuCr
146715928	HD 92499	ROAP	136.703	8231	1.34		A2SrEuCr
152808505	HD 216641	GDOR:+ROAP	119.210	6430	0.9:		FpEuCr*
153101639	*2MASS J16400299-0737293*	*ACV+ROAP+r+3h*	*151.891*	*7600*	*1.07*	*3.675*	*A7VpSrEu(Cr)*
156886111	HD 47284	ACV+ROAP+r	112.406	8294	1.37	6.856	ApSrEuCr*
158009180	*TYC 5762-828-1*	*DSCT+ROA*	*212.660*	*6280*	*1.39*		*F8*
158216369	KIC 7018170	ACV+[ROAP]+r	168.074	7000	1.15	72.747	Ap
158271090	TYC 3545-2756-1	ACV+ROAP+r+2h	84.033	7200	1.41	5.685	Ap
158275114	KIC 8677585	GDOR+ROAP+2h+s	136.975	7600	1.26		A5EuCr
159392323	TYC 3547-2692-1	ROAP	128.752	6434	0.90		F3pSrEuCr
163587609	*HD 101065*	*ROAP+s*	*118.610*	*6350*	*0.91*		*F0?V? pec*
167695608	TYC 8912-1407-1	ROAP+s	132.365	7293	1.29		F0pSrEu(Cr)
168383678	HD 96237	ACV:+[ROAP]	103.680	8119	1.33	22.842	A4SrEuCr
169078762	HD 225914	ACV:+[ROAP]+r	61.448	8100	1.72	5.242	A5VpSrCrEu
170419024	HD 151860	ROAP	73.452	7841	1.16		ApSrEuCr:
170586794	HD 107619	ACV:+ROAP	152.194	6695	0.82	10.299	F5pEuCr*
171988782	HD 258048	ROAP	169.537	6600	0.72		F4pEuCr(Sr
173372645	HD 154708	ACV+[ROAP]	180.403	7417	0.86	5.366	A2SrEuCr
174475885	HD 61622	SXARI+ROAP:	229.188	11764	2.07	0.852	B9Si
176516923	HD 38823	ACV+ROAP	165.285	7551	1.15	8.572	A5SrEuCr*

Table 1. Continued.

TIC	Name	Var Type	ν (d^{-1})	$T_{\rm eff}$ (K)	$\log \frac{L}{L_\odot}$ (dex)	$P_{\rm rot}$ (d)	Sp Type
176941102	HD 106563	DSCT/ROAP	65.460	9150	1.15		A3m:
178575480	HD 55852	ACV+ROAP:	207.181	8018	1.10	4.775	A0SrEuCr
179193226	*HD 122570*	*DSCT/ROA*	*99.120*	*9150*	*1.40*		*A3/5III:*
189996908	HD 75445	ROAP	159.116	7364	1.26		ApSrEuCr:
203817942	*HD 147911*	*DSCT/ROAP:*	*68.520*	*9900*	*0.76*		*A0Vm*
206477008	HD 24426	GDOR+ROA:	171.795	6765	0.54		F5V
211404370	HD 203932	ACV:+ROAP+r+s	242.330	7544	1.02	6.419	A5SrEu
217302172	HD 156623	DSCT+ROA	63.700	8390	1.23		A1V
220073982	HD 288081	ROT+ROA+r:	73.103	8832	1.48	0.307	A2
224284872	TYC 577-322-1	DSCT/ROA	60.47	9150	0.52		A3
237336864	HD 218495	ACV+ROAP+r+s	195.370	8283	1.03	4.200	A2EuSr
258178726	*BD+25 3139*	*DSCT/ROA*	*105.120*	*7400*	*1.41*		*F0*
259587315	HD 30849	ACV+ROAP+r	80.444	8031	1.54	15.866	ApSrCrEu
260751881	TYC 9131-119-1	ACV+ROA+2h	92.753	8614	1.20	1.197	A5m:
262590112	*TYC 577-322-1*	*DSCT/ROA*	*60.420*	*8650*	*1.31*		*A5*
264509538	KIC 10685175	ACV+ROAP+r	191.514	8355	0.97	3.103	Ap
268460597	HD 52264	ACV+ROAP:	192.139	10400	2.80	7.817	B0Si
268751602	HD 12932	ROAP+2h	124.096	7536	1.2:		ApSrEuCr
272598185	KIC 10483436	ACV+[ROAP]+r	116.899	7789	1.35	4.304	kA5hA7mA9SrCrEu
273777265	KIC 6631188	ACV+ROAP+r	129.038	7700	1.20	2.516	Ap
279485093	HD 24712	ACV+ROAP+r	235.064	7246	0.92	12.681	kA5mF0V?Sr
280198016	HD 83368	ACV+ROAP+r+4h+s	123.025	7784	1.28	2.852	A8VSrCrEu
284377321	HD 138334	ROT+ROA	86.376	7320	1.14	1.523	A0V
286992225	TYC 2553-480-1	ROAP	235.540	7487	0.93		A9pSrEu
293265536	*TYC 4-562-1*	*ROAP*	*150.250*	*7300*	*1.29*		*A9pSrEu(Cr)*
294266638	BD-19 2553	ROT+ROAP	140.730	7212	1.08		ApSrEu*
294769049	HD 161423	ACV+ROAP:	195.303	8385	1.19	10.458	ApSrEu(Cr)
299000970	*HD 176232*	*ACV+ROAP*	*125.099*	*7776*	*1.41*	*6.050*	*A4pSrEuMn*
302296720	HD 203144	DSCT+ROT+ROA	82.832	7465	0.84	0.393	A5/7V
302602874	TYC 2488-1241-1	ACV+ROAP+r	197.262	7800	1.26	3.093	A6pSrEu
308307808	CD-60 2021	DSCT+ROA	63.293	8310	1.22		A3:
310817678	HD 88507	ACV+ROAP+r	104.136	8364	1.33	2.750	ApSrEuCr:
315098995	HD 84041	ACV+ROAP+s	95.989	7730	1.34	3.696	ApSrEuCr
317719322	HD 40098	DSCT+ROA	60.186	8990	1.24		A2/3V
318007796	HD 190290	ACV+ROAP+r	196.330	7557	1.01	4.041	A0EuSr
322732889	HD 99563	ACV+ROAP+r+2h	134.238	7707	1.32	2.900	F0Sr
326185137	HD 6532	ACV+ROAP+r+2h	207.032	8383	1.22	1.945	ApSrCrEu
335303863	*HD 137949*	*ACV+ROAP+4h*	*174.079*	*8121*	*1.14*	*7.200*	*kA9hA5pSrCrEu*
340006157	HD 60435	ACV+ROAP+r+2h+s	116.857	7860	1.27	7.679	A3SrEu
342624968	HD 207561	[ROAP:]+s	240.000	7200	1.08		F0IIIm
348717688	HD 19918	ROAP+2h*+s	130.475	7400	1.23		ApSrEuCr
349945078	HD 57040	ACV+ROAP+r	183.719	8375	1.15	13.473	A2EuCr
350146296	HD 63087	ACV+ROAP+r	304.404	7753	0.97	2.664	F0pEuCr
354619745	*HD 201601*	*ACV+ROAP+s*	*117.901*	*7598*	*1.16*	*1785.700*	*A7pSrCrFe*
363716787	HD 161459	ACV+ROAP	119.838	8013	1.19	5.974	A2EuSrCr
368866492	HD 166473	ACV:+ROAP	163.460	6390	1.18	3.48:	A5SrEuCr
369845536	2MASS J19400781-4420093	ACV+ROAP+r	176.391	7868	1.33	9.529	F2(p Cr)
371800781	TYC 9311-73-1	ACV:+ROAP	62.540	8737	1.07	0.869	A4m
375937924	*TYC 525-2319-1*	*DSCT+ROAP*	*104.860*	*9150*	*1.49*		*A3m:*
380651050	HD 176384	ROT+ROA	162.234	6490	0.4:	4.184	F0/2V
380729861	*TYC 297-328-1*	*DSCT/ROAP*	*68.990*	*8900*	*3.91*		*A4m*
383521659	*HD 137909*	*ACV+ROAP*	*83.549*	*8478*	*1.39*	*18.487*	*kA8hF0pSrCrEu*
387115314	CPD-77 1337	ROT+ROA	117.178	7972	1.18	5.264	A5
394124612	HD 218994	DSCT+ACV+ROAP	98.870	7451	1.50	11.647	A3Sr
394272819	HD 115226	ACV+ROAP+r	132.590	8916	1.29	2.989	ApSrEu:
396749572	*2MASS J21553126+0849170*	*DSCT/ROA*	*61.340*	*9150*	*1.80*		*A3*
399665133	BD+06 763	ROT+ROA	71.101	8532	1.30	0.447	A2
402546736	HD 128898	ACV+ROAP+r	210.995	7463	0.74	4.480	A7VpSrCrEu
407661867	HD 37584	ROT+ROA	64.063	8657	1.24	0.562	A3V

Table 1. Continued.

TIC	Name	Var Type	ν (d^{-1})	$T_{\rm eff}$ (K)	$\log \frac{L}{L_\odot}$ (dex)	$P_{\rm rot}$ (d)	Sp Type
407929868	*HD 24355*	*ACV+ROAP+r*	*224.294*	*8235*	*1.16*	*27.916*	*A5VpSrEu*
411247704	*HD 196470*	*ROAP*	*133.402*	*7120*	*1.17*		*A2SrEu*
413938178	*HD 148593*	*ROAP*	*134.784*	*7120*	*1.30*		*A2Sr*
420687462	*HD 122970*	*ACV+ROAP+s*	*129.816*	*7400*	*0.86*	*3.877*	*F0CrEuSr*
431380369	HD 20880	ACV+ROAP+r+s	74.350	8629	1.56	5.197	ApSr(EuCr)
432223926	*HD 134214*	*ACV+ROAP+2h+s*	*254.621*	*7650*	*0.95*	*248.000*	*F2VpSrCrEu*
434449811	HD 80316	ACV+ROAP+r	194.552	8106	1.14	2.088	ApSr(Eu?)
439399707	HD 225186	ROT+ROA	60.079	7900	1.04	1.661	A3V
445543326	*HD 12098*	*ACV+ROAP+r*	*187.808*	*7152*	*1.10*	*5.460*	*F0Eu*
465996299	*HD 177765*	*ROAP*	*60.998*	*8650*	*1.69*		*A5SrEuCr*
466260580	TYC 9087-1516-1	ROT+ROAP	115.802	6099	0.72	0.695	ApEuCr*
468912168	HD 26400	DSCT/ROAP	68.223	8150	1.14		A3m:
469246567	HD 86181	ACV+ROAP+r	232.770	7223	1.11	2.051	F0Sr

ical regions of the δ Sct and γ Dor stars as determined by Balona (2018a) from *Kepler* data. The top panel shows stars in which only high frequencies are present in roAp and roA stars. The middle panel shows δ Sct stars in which one or more independent frequency peaks exceeding $60\,d^{-1}$ are present. The bottom panel shows δ Sct stars with high frequency peaks in the range 50–$60\,d^{-1}$ (high-frequency δ Sct stars, DSCTHF).

4 δ SCUTI STARS WITH HIGH FREQUENCIES

The first δ Sct star which also pulsates with roAp-like frequencies, HD 218994, was discovered by González et al. (2008). However, the high frequencies may originate in the Ap primary of a visual double with a δ Sct secondary (Kurtz et al. 2008). Quite a number of high-frequency metallic-lined (Am) stars have been identified in a photometric survey by Holdsworth et al. (2014). Some are δ Sct stars with high frequencies, but others just have isolated high frequency peaks in the roAp range.

As pointed out by Holdsworth et al. (2014), at the spectral classification resolution there is often not always a clear distinction between Am and Ap stars, so it is possible that the latter might turn out to be Ap. For this reason, Am stars with independent frequencies greater than $60\,d^{-1}$ are classed as roAp stars in Tables 1 and 2.

It is possible to obtain high frequencies in δ Sct stars due to non-linear interaction between two or more lower frequencies (the parent frequencies). If ν_1 and ν_2 are parent frequencies, then a combination frequency of the form $\nu = m\nu_1 + n\nu_2$ could be generated where m and n are positive or negative integers. By using arbitrarily large values of $|m|$ and $|n|$ it is usually possible to obtain a combination which matches any desired frequency. Identifications of this sort carry very little confidence. For this reason, the maximum values of m and n were restricted to $|n| \leq 7$, $|m| \leq 7$. If no combination is found which matches a significant frequency peak with $\nu > 60 d^{-1}$, then the star is classified as a δ Sct+roA hybrid (or δ Sct+roAp if the star is chemically peculiar). In Tables 1 and 2 these are represented as DSCT+ROA or DSCT+ROAP.

On the other hand, if the high frequency peak can be matched by a combination of lower frequencies, then the star is classified as DSCTHF (δ Scuti star with high frequencies). In fact any δ Sct star with significant frequencies higher than $50\,d^{-1}$ is classified as DSCTHF as long as there are no independent frequencies in excess of $60\,d^{-1}$ (in which case it is classified as DSCT+ROA). The limit of $50\,d^{-1}$ is arbitrary, but it has some justification in being the limit of instability predicted by non-rotating models in which driving is a result of the κ mechanism operating in the HeII partial ionization zone (see Balona et al. 2015).

The question arises as to whether δ Sct stars with independent frequencies higher than $60\,d^{-1}$ should be counted among the roA or roAp variables. Unstable modes with high frequencies are found in models of hot δ Sct stars near the ZAMS. Thus one may expect the DSCTHF stars to be found in that region of the H-R diagram. If the DSCT+ROA stars are simply DSCTHF stars, then they will also be expected to be found in the same region.

The middle panel of Fig. 3 show the location of the DSCT+ROA (including DSCT+ROAP) stars in the H–R diagram. The bottom panel shows the location of the DSCTHF stars. Both groups seem to lie near the zero-age main sequence and it would appear that DSCT+ROA(P) stars are in the same state of evolution as the DSCTHF stars. On the other hand, the roA and roAp stars without δ Sct pulsations are more widely scattered.

The top panel of Fig. 3 also shows that the ROA stars seem to extend further beyond the cool edge of the δ Sct instability region than the ROAP stars. There are two questions that can be asked: (i) is it possible that these cool ROA stars are, in fact, solar-like oscillators and (ii) if not, why are they cooler than the roAp stars?

In solar oscillations, the high-frequency peaks form a nearly equidistant set with Gaussian envelope, quite unlike the single peaks that are seen. Furthermore, the stellar luminosity derived from the observed frequency and the scaling laws for solar-like oscillations (Kjeldsen & Bedding 1995) is

Table 2. List of new roAp/roAp-like stars. The columns are the same as in Table 1.

TIC	Name	Var Type	ν (d^{-1})	$T_{\rm eff}$ (K)	$\log \frac{L}{L_\odot}$ (dex)	$P_{\rm rot}$ (d)	Sp Type
919245	HD 77746	ROA	229.681	7778	1.53		A5
3891160	HD 99120	DSCT+ROA	74.947	8614	1.21		A1V
4154746	HD 294001	DSCT+ROA	61.945	8490	1.12		A2
9171107	TYC 2479-429-1	ROT+ROA	132.107	6523	0.1:	3.096	
9176012	HD 26278	DSCT+ROA	64.395	9079	1.39		A0
9381034	HD 31100	DSCT+ROA	76.278	8629	1.24		A2
21024812	HD 14522	ACV+ROAP	95.265	7942	1.47	13.158	A8VSrEuSi
25676603	BD+27 4042	ACV+ROAP	157.205	6569	0.60	5.495	F0SrEu
26833276	HD 10682	ACV+ROAP	136.786	6967	0.81	10.417	F0VpSr
30965889	CPD-44 3294	ROA	60.968	8773	1.33		A0
31148852	CD-46 4837	ROA	61.011	8587	1.16		A2V
31817072	HD 22085	DSCT+ROA:	175.010	7122	1.54		A8/F2
32763133	HD 38629	DSCT+ROA	71.501	8674	1.18		A3V
33604636	HD 42605	ACV+ROAP	108.633	8283	1.41	2.778	ApSrEuCr
34197596	HD 25674	DSCT+ROA	132.344	8255	1.16		A1V
38846883	TYC 9138-11-1	ROA	271.424	6277	0.50		
43135807	HD 116856	ROA	78.231	6161	0.67		G0III
47005100	TYC 5469-1067-1	ROT+ROA:	207.238	6629	0.0:	3.195	
50656687	HD 36117	ROT+ROA:	86.170	7655	1.30	1.484	A2Va
53743451	HD 50711	DSCT+ROA	119.472	9291	1.38		A1/A2V
54449487	HD 137350	DSCT+ROA	114.022	8965	1.33		A2Vn:
65435735	HD 17392	DSCT+ROA+ROT	66.156	8247	0.91	9.709	A1IV
67164474	HD 40245	DSCT+ROA	66.650	8247	1.16		A2
68191357	HD 172585	ROA+ROT	63.018	8497	1.20	5.917	F
70793817	TYC 4102-1382-1	ROA:	251.831	6404	0.34		
71148851	HD 233534	ROA+ROT	65.543	7762	1.19	2.967	A2
72392575	HD 225578	ACV+ROAP	135.944	7565	1.05	3.922	A5Sr?
74288349	HD 78928	DSCT+ROA	122.978	7749	0.90		A6/8IV/V
76330671	HD 80817	DSCT+ROT+ROA	83.043	8769	1.29	2.907	A0V
76658897	HD 135449	ROT+ROAP:	152.308	6863	0.43	1.821	F/GmA9
76706808	HD 135619	DSCTHF+ROA+ROT	62.032	8467	1.08	2.967	A2IV
77270956	HD 17053	DSCT+ROA	70.990	8882	1.24		A0V
77454744	HD 17555	DSCT+ROT+ROA	82.681	8394	1.63	1.431	A0V
80542072	HD 67804	ROA+ROT+FLARE	62.978	6176	1.13	1.634	A2/3IV
81297869	HD 68695	DSCT+ROA	65.172	9125	1.31		A0Ve
91224991	HD 191380	ROA+2h	100.213	6712	0.96		F8
91257101	HD 197269	GDOR+ROA:	167.487	6711	0.91		F2V
93270207	HD 73904	ROA	79.244	9229	1.32		A2VhA0?n
93326464	HD 101523	DSCT+ROA	62.024	8985	1.17		A3V
94945153	HD 21383	DSCT+ROA:	323.781	9381	1.34		A1V
101403577	HD 189609	ROT+ROA	64.367	7975	0.97	2.079	A1V
101624823	HD 100598	ROT+ROA	124.568	6776	1.09	4.049	F0
104642645	HD 159595	DSCT+ROA	72.123	8360	1.20		A1IV/V
120532285	HD 213258	ROA	192.349	7205	0.96		Fp
123551984	HD 39929	DSCT+ROA	99.752	9018	1.21		A1V
123846458	HD 41085	DSCT+ROA	64.940	9085	1.36		A0V
124035468	HD 41878	DSCT+ROA+ROT	69.527	8991	1.28	8.130	A0V
124429243	HD 42915	DSCT+ROA	294.902	8665	1.20		A3V
125172890	HD 68619	ROT+ROA:	145.200	7737	1.16	5.952	A8/A9V
129820552	BD+36 467	ACV+ROAP	173.928	7742	0.99	6.211	ApSrEu
130089926	HD 15512	DSCT+ROA	67.591	8582	1.14		A2V
132698366	HD 65966	DSCT+ROA	73.799	8948	1.22		A3IV/V
132923245	CD-41 3649	ROA+FLARE	78.000	8124	1.27		B9
134470242	HD 55769	DSCT+ROA+ROT	67.559	8914	1.26	3.311	A2V
134860590	HD 68625	ROA+ROT	61.326	9002	1.26	3.861	A2V GAIA
137965363	HD 20725	DSCT+ROA	134.556	7809	1.15		A2
140150083	HD 71722	DSCT+ROA	72.830	9134	1.36		A0V
142889338	HD 21635	DSCT+ROA+ROT	67.553	8144	1.36	1.144	A1IV-V
143400338	BD-03 2896	ROA:	167.650	6253	0.77		F0:
144596888	HD 21997	DSCT+ROA	62.237	8406	1.09		A3IV/V
148904850	HD 137119	DSCT+ROA	63.254	8300	1.21		A2V
149630824	CD-60 1290	DSCT+ROT+ROA	73.279	7467	1.08	4.184	
149668941	AG-00 1256	ROA	255.424	6266	0.43		F8
150227188	HD 82380	ROA	165.719	8414	1.28		A4:V:
156077812	TYC 8030-11-1	ROT+ROA	183.512	5971	0.12	11.905	
156712563	HD 50471	DSCT+ROA	65.800	8894	1.23		A2/3V
156810780	HD 51093	ROA	61.667	9097	1.27		A1V
157542967	HD 171945	ROT+ROA+r	61.051	8788	1.37	0.384	A2
159195919	HD 128360	ROA+ROT	64.081	7240	1.16	1.669	A1V
159719806	HD 182952	DSCT+ROA	79.323	8900	1.14		A1V
165052884	HD 51561	ROT+ROA	188.069	7711	0.85	17.857	A5
172356142	HD 46399	ROT+ROA	61.024	6047	1.07	2.004	A2V

Table 2. Continued.

TIC	Name	Var Type	ν (d^{-1})	$T_{\rm eff}$ (K)	$\log \frac{L}{L_\odot}$ (dex)	$P_{\rm rot}$ (d)	Sp Type
173082020	HD 104366	ROA	67.910	8467	0.88		A3Vp
185163987	HD 72916	ROT+ROA	63.706	8731	1.17	10.989	A3V
192970685	HD 67871	ROT+ROA	61.222	7869	1.39	0.731	A2V
193726603	HD 162935	DSCT+ROA	83.150	8289	1.13		A3
193808452	BD+42 3743	ROA	224.721	8964	3.37		A2II
200440270	HD 30204	EA+DSCT+ROA	60.660	7147	1.24		A2IV/V
202435446	HD 2055	DSCT+ROA	74.507	8178	1.10		A0
206476784	TYC 8070-621-1	ROA	149.077	6181	0.52		
206481548	HD 209719	ROT+ROA	62.860	8139	1.14	1.125	A1IV/V
211275527	HD 189028	ROT+GDOR+ROA	109.611	7020	0.95	0.669	A9V
216904777	HD 156189	DSCT+ROA	122.571	7900	1.17		A3III/IV
231583834	HD 72248	ROT+ROA:	89.045	9002	1.24	5.747	F0V
231966653	TYC 106-1344-1	DSCT+ROA	102.540	8384	1.11		
233200244	HD 161846	ROT+ROA+r	124.471	8218	1.40	7.299	A3
233398254	HD 191490	ROT+ROA	83.931	9053	1.27	3.049	A2
237253009	TYC 4457-1700-1	ROT+ROA:	232.040	7284	0.70	10.309	
238490856	HD 67659	DSCT+ROA	61.342	8123	1.11		A5/7V
238594771	HD 68245	DSCT+ROA	61.735	8636	1.17		A2III/IV
238597976	CPD-48 1491	DSCT+ROA	61.249	8886	1.22		A2
241065253	BD+48 433	DSCT+ROA	86.459	8868	0.29		
248439776	HD 293856	DSCT+ROA	287.901	8379	1.00		A3
251026496	HD 275990	DSCT+ROA	130.482	7573	0.73		F5
255988376	HD 158952	ROT+ROA	73.386	8697	1.24	12.500	A0V
257168451	BD+00 2086	ROA	63.038	8501	1.14		A2
258626846	TYC 4451-487-1	ROT+ROA	61.364	7793	1.09	3.584	
259017938	HD 210684	ROT+ROA+r	116.825	7568	1.33	5.102	F0
262579988	TYC 220-262-1	ROA	95.547	6232	0.40		
264460765	HD 290332	DSCT+ROA	63.056	7353	0.99		A5
266806814	HD 62526	ROA+ROT	190.441	8682	1.24	12.821	A0
268911095	HD 64405	DSCT+ROA+ROT	60.979	8483	1.27	0.266	A1/3V
270319258	HD 159543	DSCT+ROA+ROT	62.317	8566	1.44	4.717	A2Vn
279248134	TYC 8541-495-1	DSCT+ROAP	64.408	8701	1.15		
283869781	TYC 2039-154-1	ROA:	258.415	6253	0.13		
285009231	HD 84320	DSCT+ROA	93.711	8188	1.10		F0
285027836	HD 65894	DSCT+ROA	62.271	8699	1.18		A1/2III/IV
286672270	HD 70369	DSCT+ROA:	113.890	7301	0.95		F5/7IV/V
286760054	HD 86976	ACV+ROAP	101.093	8255	1.56	3.979	ApSrCrEu
287636619	TYC 9201-1206-1	ROA	243.548	6472	0.56		
288242217	HD 158012	ROT+ROA	69.212	7480	1.55	5.051	F0
289486492	HD 65303	DSCT+ROA	70.526	8713	1.35		A2
293969331	TYC 8554-1868-1	ROA	198.244	6356	0.93		
295254609	HD 163362	ROT+ROA	74.176	8281	1.28	166.667	A2V
298052991	BD+78 451	ROT+ROA	197.951	7596	0.93	10.638	A2
300844158	HD 189388	DSCT+ROA	75.924	8978	1.38		A2V
306733469	HD 160721	ROT+ROA:	135.408	8173	1.87	5.208	A2III/IV
306931346	HD 69308	DSCT+ROA	69.157	8337	1.17		A3V
307606851	HD 135344	ROA	79.938	8573	1.25		A0V
309711491	HD 71340	DSCT+ROA	60.974	8436	1.17		A4V
313261813	HD 119476	GDOR+ROT+ROA	79.115	8770	1.33	0.442	A1.5V
316905967	HD 172500	DSCT+ROA	62.855	8308	1.10		A0
318944412	TYC 51-143-1	ROT+ROA	95.950	6293	-0.10	3.077	F7/8V
319740524	HD 182396	ROT+ROA	70.022	8673	1.2:	2.890	A2V
328700272	HD 122705	DSCT+ROA	80.532	8290	1.14		A4V
334009522	HD 38513	DSCT+ROA	62.267	8256	1.28		A5
335457083	HD 48409	ROT+ROA+r	180.075	8510	1.11	2.907	A3
336777433	HD 5481	DSCT+ROT+ROA	119.565	6939	1.10	0.484	A5
340559356	CD-59 1701	DSCT+ROA	67.981	8229	1.12		
348895477	TYC 8916-1634-1	DSCT+ROA	90.632	8151	1.50		
352500942	HD 221025	DSCT+ROA	71.751	8754	1.14		A2
352787151	BD+35 5094	ROAP	60.138	6912	1.57		F0SrEu
354792288	BD+48 944	DSCT+ROA	72.845	8849	1.15		A5V?
355281777	HD 56663	ROT+ROA	68.121	8887	1.24	4.149	A1/2V
358289524	HD 26564	ROA	63.282	8691	1.35		A1V
358464975	CPD-60 933	ROA+GDOR	66.671	8675	1.28		A2
358466724	CPD-60 936	DSCT+ROA	87.594	7569	1.30		A2
359030908	HD 104956	ROA	206.915	6126	0.34		F8
360020620	HD 190833	GDOR+ROT+FLARE+ROA	64.928	9900	1.28	0.568	A0V
361861044	HD 145689	DSCT+ROA	60.944	8568	1.15		A4IV-V
362351038	HD 140498	ROA	70.091	8331	1.18		A0V
372786075	HD 19984	DSCT+ROA	95.448	8114	1.05		A4V
375146283	TYC 8096-1254-1	ROT+ROA:	83.671	6365	0.69	9.668	
376717721	HD 183455	DSCTHF+ROA	66.004	8926	1.19		A2/3Vs

Table 2. Continued.

TIC	Name	Var Type	ν (d^{-1})	$T_{\rm eff}$ (K)	$\log \frac{L}{L_\odot}$ (dex)	$P_{\rm rot}$ (d)	Sp Type
376942777	HD 274350	ROA	81.453	6733	1.01		F2
377777715	HD 305125	DSCT+ROT+ROA	63.607	9400	1.35	0.370	A2
383657251	HD 77422	ROA+ROT	62.325	8760	1.19	1.603	A3V
383704522	HD 129912	ROA	203.033	6434	0.72		F3V
389297701	HD 191888	ROT+ROA	296.146	6999	0.66	3.817	F5V
389357014	HD 107174	DSCT+ROA	199.477	8412	1.14		A0
391333587	HD 93424	DSCT+ROA	64.148	8788	1.16		A4IV
394860395	BD+35 3616	ACV+ROAP	101.949	7168	1.40	6.667	F0SrEu
398476730	HD 104125	ROT+ROA	69.088	7812	1.33	1.280	A2V
404048283	HD 344097	DSCT+ROA	113.451	8714	1.07		A0
405892692	BD+49 3179	ROT+ROA	101.159	7230	0.84	0.383	F0
410163387	HD 76276	GDOR+ROAP	123.686	7697	1.58		A0SrCrEu
410350737	HD 86929	DSCT+ROA	75.263	8851	1.19		A1V
410732825	HD 21345	DSCT+ROA	88.029	8138	1.19		A5Vn
416575322	BD+48 2060	ROT+ROA	227.479	6170	0.47	10.000	F8
418424959	HD 117447	DSCT+ROA:	331.083	8238	1.21		A2/3Vn
420126478	HD 213595	DSCT+ROT+ROA	86.986	8621	1.34	0.312	A2V
427398460	HD 294239	ROA	83.515	8772	1.27		B5
427400331	HD 290662	ACV+ROAP	75.050	7418	1.4:	0.943	A0Vp
435263600	HD 218439	GDOR+ACV+ROAP	94.796	9400	0.93	3.106	A2p:Sr:Cr:Si:
436844522	HD 16729	DSCT+ROA	64.799	8487	1.17		A0
438702139	HD 116434	DSCT+ROA	130.832	8840	1.34		A2V
439915712	HD 19247	ROT+ROA	192.119	6325	0.92	9.346	F8
442896389	HD 34995	ROT+ROA	174.274	6717	0.62	3.759	F2V
444006544	HD 74911	GDOR+ROA	63.549	7950	1.48		A2IV
445493624	HD 11948	ACV+ROAP	105.857	8344	1.42	7.333	A5SrEu
450851808	HD 98435	ROT+ROA	63.945	7394	1.36	2.976	A1/2V
453826702	HD 22032	ACV+ROAP+r	139.102	7602	1.23	4.854	A3SrEuCr
455035702	HD 29182	DSCT+ROA	118.319	8249	1.09		A0
456673854	HD 59702	ACV+ROAP+r	273.822	8100	1.07	5.435	A7pSrEu
457191898	HD 24817	DSCT+ROA	101.293	8820	1.33		A2Vn
457231985	HD 290413	DSCT+ROA	120.100	8759	1.25		A0
458107917	HD 305361	DSCT+ROA	60.671	8741	1.28		A2
458536977	HD 303162	EA+DSCT+ROA	60.145	8573	0.96		A2
458622541	BD+10 1772	ROA:	107.602	6063	1.00		F8
459762136	HD 77727	ROT+ROA	185.523	5939	0.16	10.526	F8
459960597	HD 30222	DSCT+ROA	63.686	8124	1.11		A0
459976473	TYC 4191-1563-1	DSCT+EA+ROA	60.973	8221	1.10		
461230237	HD 117382	DSCT+ROT+ROA+r	63.752	8917	1.41	0.349	A1V
464470984	HD 90434	ROT+DSCT+ROA	66.495	9357	2.0:	0.653	B9IV/V
464740586	HD 302881	ROA	67.454	8511	1.12		A2
464807201	HD 29839	ROA+ROT	78.447	7956	1.67	5.682	A1V
468189624	HD 200526	DSCT+ROA	73.742	9162	1.34		A2/3V
630844439	HD 10581	GDOR+ACV+ROAP	289.721	7018	1.16	1.664	A8m

Table 3. Bright ROA stars discovered from *TESS* photometry.

TIC	Name	Var. Type	V	Sp. Type
313261813	HD 119476	GDOR+ROT+ROA	5.85	A1.5V
398476730	HD 104125	ROT+ROA	6.76	A2V
150227188	HD 82380	ROA	6.78	A4:V:
259017938	HD 210684	ROT+ROA+r	7.37	F0
359030908	HD 104956	ROA:	7.50	F8
71268401	HD 58985	ROT+ROA:	7.61	A3

not at all correlated with the stellar luminosity derived from the *Gaia* parallax. Therefore the observed frequencies are not a result of solar-like oscillations.

None of the roA stars cooler than the cool edge of the δ Sct instability strip are known to be chemically peculiar. Further observations would be desirable to confirm this result. Perhaps chemical peculiarities are more difficult to distinguish for stars as cool as 6000 K. On the available evidence, there is no reason to suspect that the nature of the high-frequency pulsations in these cool roA stars is any different from that in roAp stars.

5 Ap STARS WITH δ SCUTI PULSATIONS

Saio (2005) performed a non-adiabatic analysis of axisymmetric nonradial pulsations in the presence of a dipole magnetic field for a model with $M = 1.9\,M_\odot$ in which convection was suppressed in the stellar envelope. It was found that δ Sct pulsations are damped if the polar field strength is larger than about 1 kG. However, high-order p modes with frequencies corresponding to roAp stars driven by the κ mechanism in the HI ionization zone remain overstable even in the presence of a strong magnetic field. This analysis suggests that roAp pulsations should not co-exist with δ Sct pulsations in Ap stars unless the magnetic field strength is lower than about 1 kG.

More recent calculations by Murphy et al. (2020) indicate that the fundamental mode can be excited even in the presence of a magnetic field as strong as 4kG, but high-order g modes typical of γ Dor pulsations are strongly suppressed. The mean longitudinal field strength measured in 424 Ap/Fp stars is $\langle B_z\rangle = 890 \pm 70$ G. Among these are 10 δ Sct Ap/Fp stars with $\langle B_z\rangle = 510 \pm 200$ G, the highest field strength (HD 40759) being 2 kG. The small number of measurements is insufficient to form a definite conclusion regarding the presence of low magnetic field strengths among δ Sct/γ Dor Ap/Fp stars.

Table 4. Chemically peculiar stars known to be δ Scuti or γ Doradus variables. The columns are the same as Table 1.

TIC	Name	Var Type	$T_{\rm eff}$ (K)	$\log \frac{L}{L_\odot}$ (dex)	$P_{\rm rot}$ (d)	Sp Type
2849758	HD 243007	DSCT	9033	2.14		A1Si
9211526	HD 221226	GDOR	6840	0.90		F3Sr?
9668192	*HD 143517*	*DSCT*	*9150*	*1.18*		*A3Sr*
11646496	HD 8717	DSCT+ACV	7245	1.21	2.178	A5pCr
19924794	*HD 123255*	*DSCT/ACV*	*6903*	*1.27*	*0.839*	*F0IV(Cr)*
21073591	BD+29 3448	DSCT	7611	1.64		F0pSr
24693528	HD 14944	GDOR	7522	2.24		ApEuCr:
27962331	HD 211074	DSCTHF	7939	1.11	0.376	A5pSr(Eu)
29205693	HD 87679	DSCT	7080	0.90		A9IV(pSr)
30718811	HD 33043	GDOR+ACV	7234	1.18	0.978	F0VSr
31870361	HD 22488	DSCT	7219	1.53		A3SrEuCr
38586082	HD 27463	ACV+DSCT	8700	1.54	2.834	ApEuCrSr:
39818458	HD 40759	EA+DSCT	8785	1.99	3.815	A0CrEu
40564267	HD 184471	DSCT	10000	1.78		A9SrCrEu
47557667	*HD 129052*	*DSCTC*	*9400*			*A2SrEu?*
48330947	HD 85766	DSCT	7404	1.14		ApSi:Cr:
49673974	*HD 220556*	*DSCT*	*9400*			*A2SrEuCr*
50835993	HD 71434	DSCT	7653	1.38		A2EuCrSi?
57965241	HD 168314	DSCT+ACV	9900	2.24	7.337	A0SiEuCr
61004258	HD 81009	DSCT	9164	1.63		F1pSiSrCrEu
63671517	HD 53021	DSCT+ACV	7650	2.20	3.757	B9Si
67467015	BD+36 363	GDOR	6679	1.23		F3:IVSr:
67668604	HD 7898	DSCT	7312	1.11		A7pSr
76494115	HD 81076	DSCT	7684	2.07		A2EuCr?
78562609	HD 50143	DSCT+ACV	8384	1.46	7.453	B9EuSrCr?
78784187	HD 249401	DSCT	8148	1.85		A2Si
84863628	HD 45541	DSCT	8516	1.41		A2/3VSi:
88091070	HD 192969	DSCT+EB	8381	1.30		A5pSi
93550171	HD 74169	ACV+GDOR	9271	1.52	4.601	kA0hA2mA7
98660068	HD 3326	DSCT	7439	0.93		hA5mF0pSr
116860722	HD 246726	DSCT	7573	1.19		A5SiSr
116881415	HD 3135	DSCT	7137	1.15		F3SiCr
116995376	TYC 2413-476-1	DSCT	9069	1.71		A0Sr
118573876	HD 22128	DSCT	6960	1.44		A9IVpSrEuCrMn
120598737	HD 213421	EA+DSCT	8716	1.89		A0Si?
122932611	*HD 134185*	*DSCTC*	*7400*			*F0Si*
123587926	HD 50285	DSCT+ACV	9225	2.43	1.287	A0Si
127959761	HD 35436	DSCT	8013	1.98		A1SiSr
130587035	*HD 108506*	*DSCTC*	*7085*	*1.54*		*F2V+n(Cr)*
133696007	HD 67165	DSCTHF+ACV	9900	1.87	0.876	A0Si
138239074	DM BD+41 4078	DSCT	7689	1.22		A5SiCr?
144276313	HD 221760	DSCTHF+ACV	8600	1.86	2.628	A0VpSrCrEu
145516106	HD 137732	ACV+DSCT	9496	2.50	3.794	B9Si
145888834	HD 76063	DSCT	9900			A0Si
145917186	HD 76141	DSCT+ACV	9450	1.96	2.538	A0Si
146373520	HD 91590	DSCT+ACV	7900	1.13	3.314	ApSi
149037452	HD 34460	GDOR	6441			F3III/IVSr
152086729	HD 224962	DSCT	6768	1.53		F0Sr
152355010	HD 156040	GDOR	7816	1.97		B9Si
154714788	BD+46 3884	DSCT	7042	1.29		F0pCrEu?
158484992	HD 179259	DSCT	7604	0.99		A8EuCr?
159647185	HD 182895	DSCT	7068	1.59		F2CrEu?
165011138	HD 200859	DSCT	8329	2.06		A2Si?
166351770	DM BD+35 4422	DSCT	7847	1.62		A5Si?
169971995	HD 66533	DSCT	9422	2.15		kB9hA3mA8SrCrEu
178108654	HD 20476	DSCTHF	9176	2.04		A5Si
178750406	HD 56206	ACV+GDOR	9900	2.14	4.906	A0Eu
190682740	HD 76406	DSCT+ACV	8147	2.09	2.578	A0Si
191672063	HD 77809	DSCT+ACV	7925	1.65	4.749	ApSrCr:
192375956	BD+46 681	DSCT	7681	1.80		A8VSrCrEuSi
194356599	HD 653	DSCT+ACV	10000	1.82	1.085	A0CrEu

Table 4. Continued.

TIC	Name	Var Type	$T_{\rm eff}$ (K)	$\log \frac{L}{L_\odot}$ (dex)	$P_{\rm rot}$ (d)	Sp Type
213564899	HD 338654	DSCT	7989	1.56		A0Si
231813751	HD 38471	GDOR+ACV	7650	2.12	2.429	B9Si
235676117	HD 176281	GDOR	6850	1.17		F2pSr:
237564008	HD 50345	DSCT	8833	1.55		A0EuCr
238659021	HD 8441	DSCT	9471	2.33		kB8hA3pSrCrEu
239738736	HD 247232	DSCT	9175	1.84		A2SiCr
245179731	HD 191836	DSCT	8010	1.78		A4/5IV/VSr
245641254	HD 16460	GDOR	6393	2.44		F1IV-VpSrEuCr:
245792896	*HD 28319*	*DSCTC+E:*	*8430*	*1.65*		*A9IVSr*
248354858	HD 7133	DSCT	7133	1.41		A3Sr
252906029	HD 50972	ACV+DSCT	9655	1.60	1.047	B9VSrCr
260204804	HD 131910	DSCT	6966	1.61		F4EuCr
267021905	HD 220071	DSCT+ELL	7400	0.99	0.815	A7/F0V:p:Si:(Sr?)
271057422	HD 75425	DSCT	8042			A0SrEuCr?
283613369	DM BD+35 4340	DSCT	7480	1.93		F0SiSr?
289228040	HD 200177	DSCT+ACV	9928	1.55	1.469	kA0hA2pCrSr
296375471	HD 131171	DSCT	7650	2.37		B9Si
298197561	HD 340577	DSCT	8461	2.05		A3SrCrEu
301946105	HD 7410	DSCT	7815	1.85		A5SrCrEu
303478699	HD 154253	DSCT+ACV	8001	1.51	3.094	A0SrCrEu
307642246	HD 72634	ACV+DSCT	9300	2.37	1.861	A0EuCrSr
307930890	HD 85672	DSCTHF	7850	1.00		A3VpSr
311778802	HD 39135	DSCT	8645	2.40		A0SiCrSr
312221714	HD 248727	DSCT	9790	1.93		A0MnSiCr
316520410	HD 21427	GDOR	9078	1.56		A3VSi:
320504339	HD 2852	DSCT	7835	1.97		A5SrEu
323432344	HD 32314	DSCT	8044	1.08		A5Si
324437240	HD 169594	DSCT+ACV	8328	1.95	1.649	ApCrSrSi
331644554	DM BD+46 3543	EA+DSCT	8450	1.18		A2Si
333808016	HD 62632	DSCT+ACV	8810	2.06	3.281	A2CrEu
342575976	HD 170005	DSCT	7785	1.57		A2pSr
343126267	LF 4 +55 111	DSCT	7998	1.13		F0SiSr
344177424	HD 89877	DSCT+ACV	8925	2.41	3.186	ApEuCrSr:
345426423	TYC 4004-312-1	GDOR	8217	1.52		A0Si?
348772511	HD 21190	DSCT	7028	1.63		F2IIISrEuSi:
356088697	HD 76460	DSCT	8454	1.57		ApSrEuCr*
356439350	HD 181331	DSCT+ACV	9900	2.16	3.571	A0VpSi
361168660	HD 144059	EA+DSCT	9900	2.42		A0III:
362622494	HD 147174	DSCTHF	9900	1.36		A0SiCrSr
363387100	HD 192060	GDOR	7140	1.49		A5YSr?
363550117	*HD 99458*	*EB+DSCT*	*7600*	*1.52*		*A2*
364257619	HD 191426	DSCT+ACV	9900		3.184	A0Si
371976932	HD 240242	DSCT	9400	2.05		A4Si
382631655	CPD-60 922	DSCT+ACV	7295	0.79	1.446	A0Si?
385594939	*[M67b] +23 477*	*DSCT*	*9400*			*kA2mF0SrSi*
389841228	BD+38 2360	GDOR	7042	0.86		F0pSrCrEu
393799555	HD 108283	DSCT+ACV	7170	1.76	1.272	A9IVnpSr
401529004	HD 77830	DSCT	7821	1.66		A5SrCr
408246457	HD 281886	GDOR	6547	0.66		F0pSr?
417206015	HD 205171	DSCT	9888	1.65		kA0.5mA1Vas(Si)
418241480	HD 19978	DSCT	7780	1.59		ApCrEuSr
427377135	HD 36955	DSCTHF+ACV	8057	1.60	2.283	kA0hA2mA4CrEu
429556532	*[M67b] +22 315*	*GDORH*	*7555*			*A2pSr:*
431029903	LF 4 +52 312	DSCT	7276	1.61		A3pSr
437231105	HD 95158	DSCT	7193	1.43		A7SrCr?
445325141	HD 59660	DSCT+ACV	8251	2.42	4.283	A0EuCr?
445796153	HD 34740	ACV:+DSCTHF	7351	1.19	5.576	A0pSrSi
450091404	HD 287150	DSCT	8169	1.72		A3SrCr?
452907921	*HD 66853*	*DSCT:*	*7120*			*F2IIIpSrEuCr:*
470680611	HD 195147	DSCT	6889	1.39		F0pSrSi

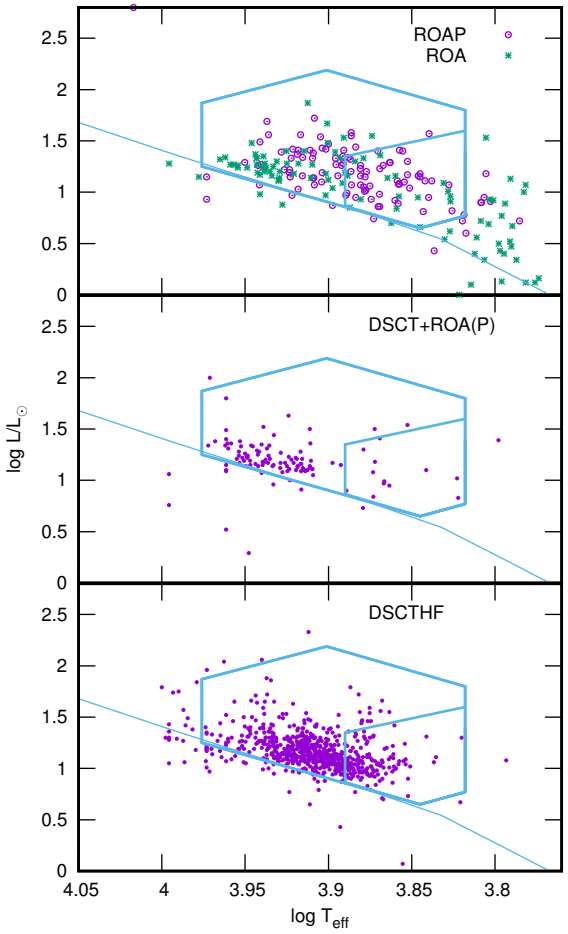

Figure 3. Theoretical H–R diagrams for roAp stars. The top panel shows roA and roAp stars. The middle panel shows δ Sct stars with at least one independent frequency in the roAp range. The bottom panel shows δ Sct stars with high frequencies not exceeding 60 d^{-1} (DSCTHF). The solid line is the zero-age main sequence from solar abundance models by Bertelli et al. (2008). The polygons are the approximate areas where most δ Scuti and γ Dor stars are to be found (Balona 2018a).

There are 121 Ap/Fp stars in which δ Sct or γ Dor pulsations are present (Table 4). Most of the Ap δ Sct stars contain high-order g modes, just like their non-peculiar counterparts. This is in contradiction to the models of Saio (2005) and Murphy et al. (2020). Four stars which may be included in this table, TIC 26418690, 394124612, 410163387 and 435263600, are listed in Tables 1 and 2 because they have frequency peaks higher than 60 d^{-1} (DSCT+ROAP or GDOR+ROAP).

To compare the relative number of pulsating Ap/Fp stars with those of normal A/F stars, only main-sequence stars brighter than 10-th magnitude and with $6000 < T_{\rm eff} < 9000$ K were selected. The magnitude limit ensures that the sample is fairly complete. With these restrictions, there are 33900 stars observed by *TESS* of which 6250 are classified as δ Sct or γ Dor. Thus about 18 percent of all main sequence stars in this temperature range are pulsating δ Sct/γ Dor variables.

In the same effective temperature and magnitude ranges, there are 472 Ap/Fp stars observed by *TESS* of

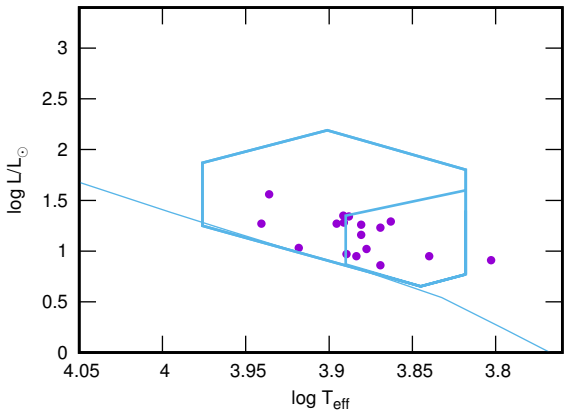

Figure 4. Location of stars with variable or broad frequency peaks in the H-R diagram.

which 41 are δ Sct or γ Dor stars. Thus among Ap/Fp stars, about 9 percent pulsate as δ Sct or γ Dor. It would seem that the relative number of these pulsating variables among the chemically peculiar stars is about half of that in the general population of main sequence stars. In the same $T_{\rm eff}$ and magnitude ranges, there are 39 *TESS* roAp stars. If one counts these among the δ Sct/γ Dor group, then about 17 percent of Ap/Fp stars pulsate.

Counting roAp stars as part of the δ Sct/γ Dor group of variables means that the relative number of pulsating stars among the Ap/Fp stars is about the same as in the general population. There is, however, a strong selection for roAp-like frequencies among the Ap/Fp stars. In other words, in order to resolve the nature of roAp stars one should perhaps be investigating the mode selection mechanism rather than a problem of different pulsation mechanisms.

Many of the δ Sct/γ Dor stars listed in Table 4 are also rotational variables as a result of chemical spots. One may have expected that, as in the roAp stars, rotational multiplets may be present. After all, they presumably all have approximately kilogauss magnetic fields which may cause the pulsation axis to be aligned with the magnetic axis. However, no convincing example of exactly equidistant frequency spacing can be found in these stars. This may be explained by the fact that only modes with spatial wavelengths comparable to the pressure scale height are likely to be affected by the strong magnetic field in the atmosphere. These would tend to be modes of high radial order. The majority of the δ Sct pulsation modes are thus not affected.

6 UNSTABLE FREQUENCIES

Variation in the pulsation frequencies and amplitudes and/or transient behaviour in roAp stars has often been reported. For example, Matthews et al. (1987) found a very complex fine structure of individual frequency peaks in the periodogram of HD 60435 which changes with time. *TESS* observations of this star show pulsations that appear and disappear in a matter of days (Balona et al. 2019). Martinez & Kurtz (1990) found long-term variations in the principal pulsation frequency of HD 101065 and transient frequencies in HD 203932 (Martinez et al. 1990). HD 101065

(Przybylski's star) seems to show a secondary high frequency which appears to vary in amplitude on a timescale of days (Ofodum & Okeke 2016).

Kreidl et al. (1991) reported a significant shift in the primary oscillation frequency of HD 217522, which was later confirmed by Medupe et al. (2015) who suggested that the pulsations may have growth and decay times shorter than a day. Kreidl et al. (1991) also found a frequency that was visible in 1982 but had disappeared in 1989. For HD 134214 Kreidl et al. (1994) found variations in the pulsation frequency over a timescale of 248 d.

Martinez & Kurtz (1994) found that the lifetimes of some of the modes in HD 84041 appear to be shorter than the rotation period. For HR 3831, Kurtz et al. (1997) found that the frequency variation cannot be explained by time delay in a binary system and must be intrinsic to the star as a result of changes in the pulsation cavity. Handler et al. (2002) reported that the previously-detected oscillations in HD 122970 had vanished and the modes that remained had slightly different frequencies and amplitudes. The presence of different peaks in TIC 167695608 at different times (Cunha et al. 2019) may also indicate a transient nature. Frequency variability in TIC 41259805 has been reported by Holdsworth et al. (2021).

Since the original discovery by Cunha et al. (2019), additional *TESS* data for TIC 350146296 (HD 63087) shows fine structure or broad peaks in five pulsation peaks (presumably consecutive radial orders) and their rotational sidelobes.

The case of HD 207561 is interesting. This star has been given spectral classifications in the range A5–F3 (non-peculiar) and is classified as Am by Bidelman (1966). It shows a distinct photometric variation with a 6-min period on two consecutive nights (Joshi et al. 2006), but further observations failed to confirm the variation. There is no indication of pulsation in the *TESS* data. Nevertheless, it is included here as it might be an example of transient pulsations.

In KIC 10483436 the main roAp pulsation is highly variable in frequency with a timescale of tens of days, though other high frequencies are stable (Balona 2013). It is remarkable that although the high frequency at $116.9\,\mathrm{d}^{-1}$ has too low an amplitude to be detected by *TESS*, the *TESS* data shows a strong peak at $7.259\,\mathrm{d}^{-1}$ (S/N = 7.0) which is not seen in the *Kepler* data. It does not seem to be an harmonic of the rotation frequency. Transient frequency peaks are not uncommon in roAp stars.

KIC 8677585 was discovered as a roAp variable by Balona et al. (2011b) from *Kepler* observations. It is interesting in having a strong peak at $\nu = 3.142\,\mathrm{d}^{-1}$ which cannot be explained except as a pulsation. It may therefore be classified as a γ Dor+roAp variable. Later, Balona et al. (2013) showed that amplitude and frequency variations were present in all frequencies and that the frequency and amplitude variations in the $3.142\,\mathrm{d}^{-1}$ peak match those of one of the roAp peaks. *TESS* observations of the same star (TIC 158275114) show the same high-frequency peaks (with considerably higher noise level), but the peak at $3.142\,\mathrm{d}^{-1}$ seems to have completely disappeared, as illustrated in Fig. 5. Instead, a new peak at a frequency of $1.000\,\mathrm{d}^{-1}$ has taken its place.

The star is not a rotational variable and it is unlikely that the new peak has anything to do with rotation. It seems that the lifetimes of even the low-frequency modes are much shorter than can be explained by current theory. Low-frequency modes of unknown origin were also detected in the roAp stars KIC 10483436 and KIC 10195926 (Balona 2013). For some reason, it seems that transient low frequencies may be connected with the roAp phenomenon.

Another roAp star with low frequencies is TIC 35905913 (HD 132205), which Kochukhov et al. (2013) discovered to pulsate at $201\,\mathrm{d}^{-1}$ from radial velocity observations. The *TESS* photometry is not sufficiently precise to detect this pulsation, but rotational modulation with $P_{\rm rot} = 7.48\,\mathrm{d}$ is seen. In addition, there are some low-amplitude peaks at $2.59\,\mathrm{d}^{-1}$ and its harmonic which are not related to the rotation.

Other roAp stars with low frequencies are TIC 156886111 (Balona et al. 2019) and TIC 119327278 with a peak at $17.783\,\mathrm{d}^{-1}$. TIC 260751881 is a roA with a peak at $8.933\,\mathrm{d}^{-1}$ is yet another example. These stars could perhaps be classified as γ Dor (GDOR) in addition to roAp or roA. However, the transient nature of the low frequencies in some stars is not seen in normal γ Dor stars.

Transient or stochastic behaviour seems to be present in about 15 percent of known roAp stars, which suggests that it might be more common than generally acknowledged. Something in the star is clearly changing, sometimes with timescales measured in days, but on longer timescales in other stars. While amplitude variation in some frequencies is not uncommon in δ Sct stars (Bowman et al. 2016), these never occur on timescales of a few days. Stochastic behaviour, as seen in HD 60435 and a few other roAp stars, has never been seen in δ Sct or γ Dor stars. This behaviour is, in fact, inexplicable in self-driven modes where the growth timescale is measured in years or centuries.

Spectroscopic, unlike photometric observations, are sensitive to depth in the atmosphere, and frequencies which are visible in the radial velocities are sometimes not seen in the photometry and vice-versa (e.g. Kurtz et al. 2006b). This might be attributed to the presence of a node at the level where photometric variations are most visible. Another possibility is that the modes visible in the spectroscopy have high spherical harmonic degree, and thus not visible in the photometry. A third possibility is that the modes detected in the radial velocities have short lifetimes. Also, significant changes in radial velocity amplitude with time are sometimes observed (Kurtz et al. 2006b). There are also large differences in radial velocity amplitude and phases in lines of different elements which could be attributed to a dependence of pulsation amplitude with height.

The location of stars with variable or broad high-frequency peaks are shown in Fig. 4. Note that they seem to be located roughly in the middle of the roAp instability region and not at the red edge where one might expect short mode lifetimes as found in solar-like oscillations.

7 THE OBLIQUE PULSATOR MODEL

It turns out that all chemically peculiar stars in Tables 1 and 2 which show rotational sidelobes also have rotationally modulated light curves (i.e. they belong to the ACV class). The converse is not true. There are 37 stars where rotational

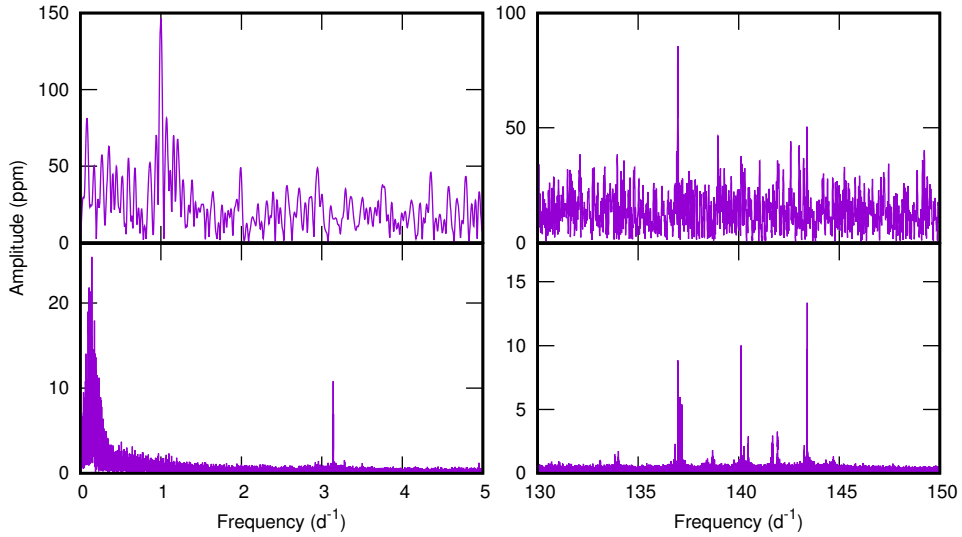

Figure 5. The top two panels show the periodogram of TIC 158275114 (KIC 8677585) observed by *TESS* in the low- and high-frequency regions. The bottom panels show the periodograms of the same star in the same two frequency regions as observed by *Kepler*.

light modulation is present, but rotational sidelobes are not seen. This may be due to a close alignment of the magnetic and rotation axes, a very long rotation period, low signal-to-noise in the periodogram or spherical harmonic degree and orientation.

In a roAp star, the pulsation axis is closely aligned with the magnetic axis. As the star rotates, the pulsation is seen from a different aspects, resulting in a variation in amplitude in the line of sight. This leads to rotational sidelobes in the periodogram which are spaced by the rotational frequency. The number and relative amplitudes of the sidelobes provides information on the spherical harmonic degree and relative inclination of the pulsation axis. This oblique pulsator model was first proposed by Kurtz (1982) and further elaborated by Kurtz & Shibahashi (1986).

In the oblique pulsator model, the angle between the rotational axis and the axis of pulsation is given by

$$\tan i \tan \beta = \frac{A^{(1)}_{+1} + A^{(1)}_{-1}}{A^{(1)}_{0}}$$

where $A^{(1)}_{\pm 1}$ are the dipole sidelobe amplitudes, $A^{(1)}_{0}$ is the amplitude of the central peak and i is the rotation inclination. This holds true under the assumption that the eigenfunction is a single, pure, spherical harmonic.

While the success of the oblique pulsator model cannot be doubted, there is one apparent exception: TIC 326185137 (HD 6532). Kurtz et al. (1996) found a frequency quintuplet spaced exactly by the rotation frequency. It was found that the dominant mode is a dipole ($l = 1$) with a small quadrupole ($l = 2$) component. Using a rotational inclination of $i = 50°$, the above formula leads to $\beta = 59°$, but other combinations are possible.

Later, the star was observed by *TESS* (Balona et al. 2019) showing only two peaks at 207.030 and 208.058 d^{-1}. These match up with two of the quintuplet sidelobes described by Kurtz et al. (1996). Although the frequency spacing between sidelobes is the same, the relative amplitudes are completely different. Since it is the relative amplitudes which provide a constraint on the geometry of pulsation, as seen in the above relationship, this implies a change in the pulsation geometry, which seems inexplicable. Indeed, Kurtz & Holdsworth (2020) suggested that either the star has changed its pulsation axis or, more likely, that the effect is due to depth dependence differences induced by the different photometric passbands.

Note, however, that the sidelobes in the *TESS* data are separated by very nearly 1 cycle/day. A severe alias problem is acknowledged by Kurtz et al. (1996) as follows: "The proximity of the rotation period to 2 d means that frequency analyses of observations obtained from a single site suffer from severe alias problems. These problems have stifled work on this star". Using data from South Africa and Australia, a more accurate rotation period was derived. Because of the aliasing problem and the long time span between data sets (1985 to 1994) they had to rely on expectations from the oblique pulsator model to choose among statistically equivalent aliases. It seems that the resolution of this problem is very simple. The severe aliasing in the ground-based observations led Kurtz et al. (1996) to mistake two aliases for real peaks. As a consequence, the true pulsation amplitudes cannot be determined.

Rotational light modulation as well as rotational sidelobes is present in TIC 220073982 (Balona et al. 2019) as well as in four new roA stars TIC 157542967, 233200244, 259017938 and TIC 335457083. It seems likely that these may be unrecognised Ap stars. However, tidal action can also give rise to rotational sidelobes (Reyniers & Smeyers 2003; Balona 2018b) and should perhaps be considered.

8 EMPIRICAL RELATIONSHIPS

Balona et al. (2019) investigated the possibility of using the radial order, n, of a pulsation mode rather than the frequency as a means of discriminating roAp stars from δ Sct variables. One could define roAp/roA stars as those having values of n greater than a certain value, for example. This is similar, but not quite the same as adopting a frequency crite-

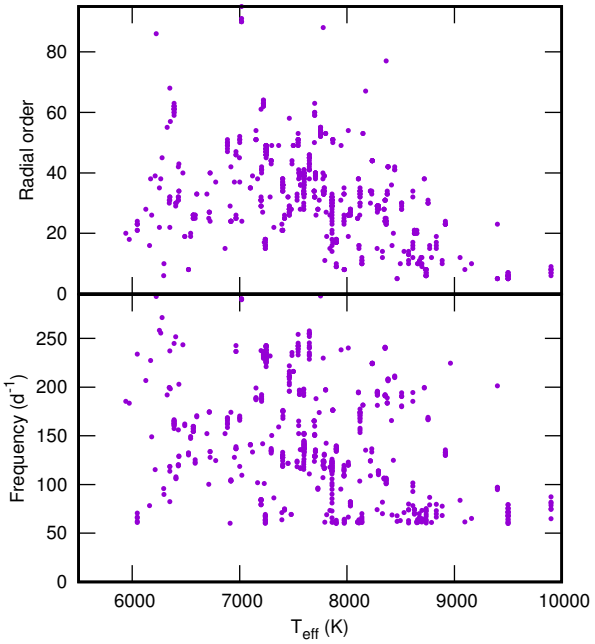

Figure 6. Top panel: the radial order, n, as a function of effective temperature for roAp or roA stars. Bottom panel: typical pulsation frequency as a function of effective temperature.

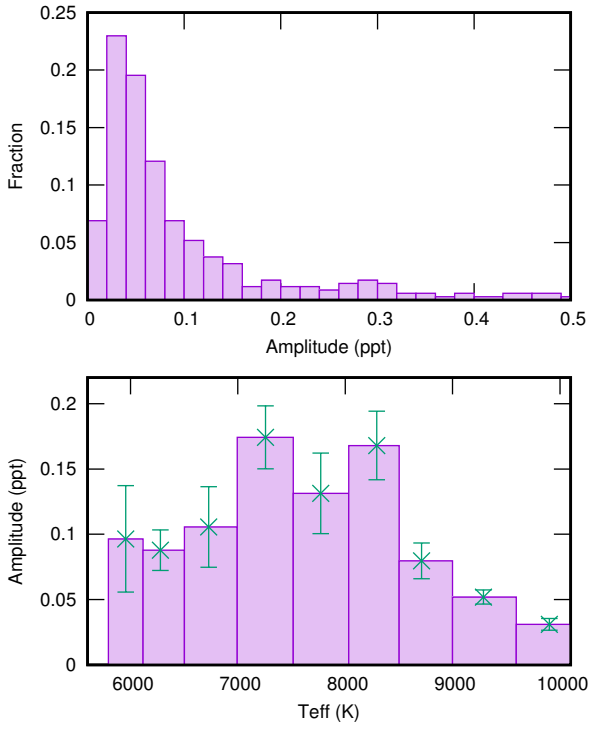

Figure 7. Top panel: the amplitude distribution (in parts per thousand) of roAp and roA stars from *TESS* observations. The bottom panel shows the *TESS* amplitude distribution as a function of effective temperature. The error bars are 1-σ in length.

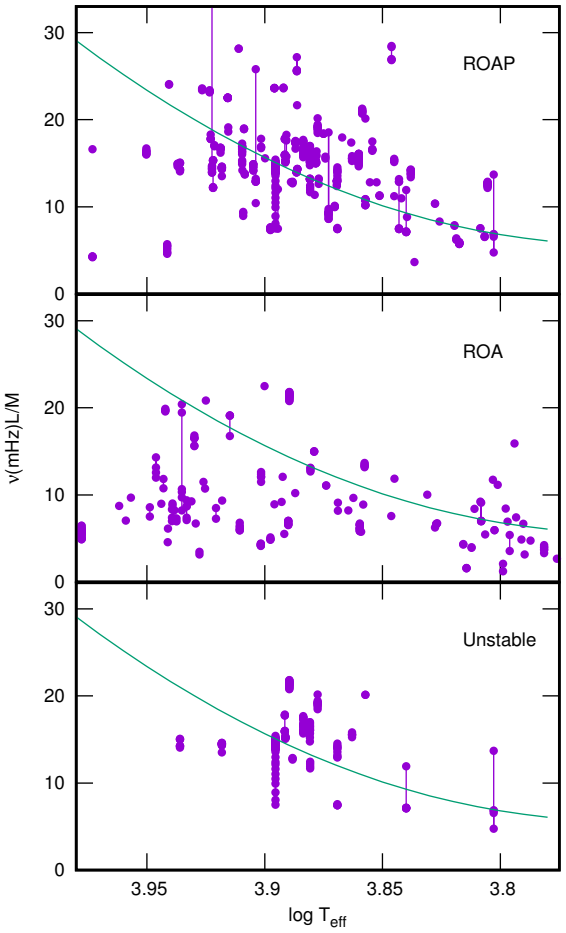

Figure 8. Top two panels: the location of the roAp and roA stars in the $\log T_{\rm eff} - \nu L/M$ plane where ν is the frequency in mHz and L, M is the luminosity and mass in solar units. Different frequencies in the same star are connected by a vertical line (harmonics ignored). The solid curve is the approximate acoustic critical frequency from models. The bottom panel shows the location of stars with unstable frequencies.

rion. The value of n associated with the pulsation frequency for each star in Tables 1 and 2 was derived from the stellar parameters and pulsation models by Dziembowski (1977). The resulting values of n as a function of effective temperature, $T_{\rm eff}$, are shown in the top panel of Fig. 6. The bottom panel shows the pulsation frequency as a function $T_{\rm eff}$. As can be seen, there is no advantage in using the radial order as a classification criterion.

Nearly all ground based observations of roAp stars were conducted using the Johnson B filter, from which 183 individual frequency amplitudes from 38 stars are available. From *TESS* observations 512 individual frequency amplitudes from 165 roAp or roA stars are available. This allows a good determination of the pulsation amplitude distribution (Fig. 7, top panel). The drop in the fraction of stars in the first bin is very likely a result of the detection limit. It is possible that many more high-frequency stars remain undetected by *TESS*.

As discussed above, there are several roAp stars observed by *TESS* in which the high frequencies are not detected. One of the reasons is that the amplitude in B is much

larger than in the *TESS* passband. Comparison of peak amplitudes of the same stars measured in the two passbands indicates that $A_B \approx 4A_T$.

In the bottom panel of Fig. 7 the distribution of mean amplitude as a function of effective temperature is shown. The largest amplitudes occur at about $T_{\rm eff} \approx 7000$–8000 K, which is also the range where most δ Sct stars are to be found and where high-amplitude δ Sct stars are located (Balona 2018a).

It has been known for a long time that the pulsation frequencies in a significant number of roAp stars exceed the acoustic critical frequency, $\nu_{\rm crit}$. This is the frequency beyond which the pulsational acoustic waves are no longer reflected in the atmosphere. Modes with $\nu > \nu_{\rm crit}$ manifest as running waves, leading to energy loss and damping of pulsational driving.

As pointed out by Saio (2014), the critical frequency is best shown in the $\log T_{\rm eff} - \nu L/M$ plane where ν is the frequency in mHz and L and M are the luminosity and mass in solar units. Fig. 8 shows the location of the roAp and roA stars in this diagram. The calculated critical frequency is adapted from Saio (2014) and Audard et al. (1998). Note that the the frequencies in about half the roAp stars exceed the critical acoustic frequency. However, for most of the roA stars the pulsation frequency is below critical. It is not clear if this is significant owing to uncertainties in the stellar parameters as well as uncertainties in the atmospheric models used to estimate $\nu_{\rm crit}$. However, it offers the suggestion that $\nu_{\rm crit}$ may have been underestimated owing to the different atmospheric structure in Ap stars.

Also interesting is the fact that stars with unstable frequencies or amplitudes do not have higher than normal frequencies (bottom panel of Fig. 8).

9 CONCLUSION

In this paper, a minimum frequency of $60\,{\rm d}^{-1}$ was selected as the criterion for the roAp class. If all frequency peaks are below this limit, the stars is classified as a δ Scuti; if above, it is classified as a roAp star. Low frequencies due to rotation or γ Dor pulsation may, however, be present. A large number of stars with apparently normal chemical composition also pass this criterion. The label "roA" is used to distinguish these from the roAp stars. It is, of course, possible that they may turn out to be Ap stars on further study.

It should be noted that the latest models of non-magnetic, chemically normal stars by Xiong et al. (2016) show that high-mass A stars are unstable at frequencies as high as $200\,{\rm d}^{-1}$. This shows that it may not be necessary to impose a high magnetic field to explain the roAp/roA pulsations. These models suggest that chemically normal stars with frequencies typical of roAp stars should exist. It would therefore be a mistake to assume, a priori, that roA stars are all mis-classified Ap stars.

In the absence of a suitable model for roAp stars, it is argued that a simple frequency criterion has no physical meaning. In fact, there are large numbers of stars with frequencies just below $60\,{\rm d}^{-1}$ and there is no compelling reason why they should not be considered as roA or roAp stars. Conversely, there is no reason why stars with frequencies just above $60\,{\rm d}^{-1}$ (or any other frequency limit) should not be classified as δ Sct stars, even if they are chemically peculiar.

It might be argued that high frequencies seem to be confined to chemically peculiar stars, in which case a separate classification is required. But even among the Ap stars, δ Sct pulsations are fairly common and the same problem arises. It turns out that about 9 percent of Ap stars are δ Sct variables, which is half the proportion among chemically normal stars. In fact, if one adds the number of roAp stars to the number of chemically peculiar δ Sct stars, the fraction of pulsating Ap stars is the same as the fraction of pulsating non-Ap stars. The models of Saio (2005) and Murphy et al. (2020), which predict that low frequencies are strongly damped in Ap stars, are in conflict with observations.

It is well-known that δ Sct stars with the same physical parameters may have completely different frequency distributions (Balona et al. 2015). This presents a severe problem in stellar pulsation and indicates that mode selection is extremely sensitive to local conditions in the upper layers of the star. One could take the view that the roAp/roA stars are just another manifestation of this unknown mode selection process. To account for the higher proportion of roAp frequencies in chemically peculiar stars, one can presume that a large magnetic field favours selection of high frequencies.

Perhaps the most puzzling aspect of roAp/roA stars is the instability of the pulsations. The roAp star HD 60435 is the most extreme example, showing a timescale of a few days in which pulsations appear and disappear (Balona et al. 2019). Variations of this sort are characteristic of solar-like oscillations.

It is possible that some of these results can be attributed to incorrect assumptions regarding the outer layers of A and B stars. Evidence for rotational light modulation, indicating the presence of starspots, shows that the radiative upper layers in A and B stars are not fully understood (Balona 2019, 2021). Under the circumstances, a solution to the cause of the high frequencies in roAp and roA stars is unlikely to be found until the problem of mode selection in the much simpler δ Sct stars has been resolved.

DATA AVAILABILITY

The data underlying this article are available in the article.

ACKNOWLEDGMENTS

I thank the National Research Foundation of South Africa for financial support and Dr Gerald Handler for useful comments.

This paper includes data collected by the *TESS* mission. Funding for the *TESS* mission is provided by the NASA Explorer Program. Funding for the *TESS* Asteroseismic Science Operations Centre is provided by the Danish National Research Foundation (Grant agreement no.: DNRF106), ESA PRODEX (PEA 4000119301) and Stellar Astrophysics Centre (SAC) at Aarhus University. We thank the *TESS* and TASC/TASOC teams for their support of the present work.

This work has made use of data from the European Space Agency (ESA) mission Gaia

(https://www.cosmos.esa.int/gaia), processed by the Gaia Data Processing and Analysis Consortium (DPAC, https://www.cosmos.esa.int/web/gaia/dpac/consortium). Funding for the DPAC has been provided by national institutions, in particular the institutions participating in the Gaia Multilateral Agreement.

This research has made use of the SIMBAD database, operated at CDS, Strasbourg, France. This research has made use of the VizieR catalogue access tool, CDS, Strasbourg, France (DOI: 10.26093/cds/vizier). The original description of the VizieR service was published in A&AS 143, 23.

The data presented in this paper were obtained from the Mikulski Archive for Space Telescopes (MAST). STScI is operated by the Association of Universities for Research in Astronomy, Inc., under NASA contract NAS5-2655.

REFERENCES

Audard N., Kupka F., Morel P., Provost J., Weiss W. W., 1998, A&A, 335, 954
Balmforth N. J., Cunha M. S., Dolez N., Gough D. O., Vauclair S., 2001, MNRAS, 323, 362
Balona L. A., 2013, MNRAS, 436, 1415
—, 2014, MNRAS, 437, 1476
—, 2018a, MNRAS, 479, 183
—, 2018b, MNRAS, 476, 4840
—, 2019, MNRAS, 490, 2112
—, 2021, Frontiers in Astronomy and Space Sciences, 8, 32
Balona L. A., Breger M., Catanzaro G., et al., 2012, MNRAS, 424, 1187
Balona L. A., Catanzaro G., Crause L., et al., 2013, MNRAS, 432, 2808
Balona L. A., Cunha M. S., Gruberbauer M., et al., 2011a, MNRAS, 413, 2651
Balona L. A., Cunha M. S., Kurtz D. W., et al., 2011b, MNRAS, 410, 517
Balona L. A., Daszyńska-Daszkiewicz J., Pamyatnykh A. A., 2015, MNRAS, 452, 3073
Balona L. A., Holdsworth D. L., Cunha M. S., 2019, MNRAS, 487, 2117
Balona L. A., Ozuyar D., 2020, MNRAS, 493, 5871
Bedding T. R., Murphy S. J., Hey D. R., et al., 2020, Nature, 581, 147
Bertelli G., Girardi L., Marigo P., Nasi E., 2008, A&A, 484, 815
Bidelman W. P., 1966, Vistas in Astronomy, 8, 53
Bowman D. M., Kurtz D. W., Breger M., Murphy S. J., Holdsworth D. L., 2016, MNRAS, 460, 1970
Cunha M. S., 2002, MNRAS, 333, 47
Cunha M. S., Alentiev D., Brandão I. M., Perraut K., 2013, MNRAS
Cunha M. S., Antoci V., Holdsworth D. L., et al., 2019, MNRAS, 487, 3523
Dziembowski W., 1977, Acta Astron., 27, 95
Elkin V. G., Kurtz D. W., Mathys G., Freyhammer L. M., 2010, MNRAS, 404, L104
Gaia Collaboration, Brown A. G. A., Vallenari A., Prusti T., de Bruijne J. H. J., Babusiaux C., Bailer-Jones C. A. L., 2018, ArXiv e-prints
Gaia Collaboration, Prusti T., de Bruijne J. H. J., et al., 2016, A&A, 595, A1
Gautschy A., Saio H., Harzenmoser H., 1998, MNRAS, 301, 31
Głębocki R., Gnaciński P., 2005, in ESA Special Publication, Vol. 560, 13th Cambridge Workshop on Cool Stars, Stellar Systems and the Sun, Favata F., Hussain G. A. J., Battrick B., eds., p. 571
Gontcharov G. A., 2017, Astronomy Letters, 43, 472
González J. F., Hubrig S., Kurtz D. W., Elkin V., Savanov I., 2008, MNRAS, 384, 1140
Handler G., Weiss W. W., Paunzen E., et al., 2002, MNRAS, 330, 153
Hey D. R., Holdsworth D. L., Bedding T. R., et al., 2019, MNRAS, 488, 18
Holdsworth D. L., Cunha M. S., Kurtz D. W., et al., 2021, MNRAS, sumitted
Holdsworth D. L., Smalley B., Gillon M., et al., 2014, MNRAS, 439, 2078
Jenkins J. M., Twicken J. D., McCauliff S., et al., 2016, in Proc. SPIE, Vol. 9913, Software and Cyberinfrastructure for Astronomy IV, p. 99133E
Joshi S., Mary D. L., Martinez P., Kurtz D. W., Girish V., Seetha S., Sagar R., Ashoka B. N., 2006, A&A, 455, 303
Khalack V., Lovekin C., Bowman D. M., et al., 2019, MNRAS, 490, 2102
Kjeldsen H., Bedding T. R., 1995, A&A, 293, 87
Kochukhov O., Alentiev D., Ryabchikova T., Boyko S., Cunha M., Tsymbal V., Weiss W., 2013, MNRAS, 431, 2808
Koen C., 2010, Ap&SS, 329, 267
Kreidl T. J., Kurtz D. W., Bus S. J., Kuschnig R., Birch P. B., Candy M. P., Weiss W. W., 1991, MNRAS, 250, 477
Kreidl T. J., Kurtz D. W., Schneider H., van Wyk F., Roberts G., Marang F., Birch P. V., 1994, MNRAS, 270, 115
Kurtz D. W., 1978, Information Bulletin on Variable Stars, 1436, 1
—, 1982, MNRAS, 200, 807
Kurtz D. W., Elkin V. G., Cunha M. S., Mathys G., Hubrig S., Wolff B., Savanov I., 2006a, MNRAS, 372, 286
Kurtz D. W., Elkin V. G., Mathys G., 2006b, MNRAS, 370, 1274
Kurtz D. W., Holdsworth D. L., 2020, Astrophysics and Space Science Proceedings, 57, 313
Kurtz D. W., Hubrig S., González J. F., van Wyk F., Martinez P., 2008, MNRAS, 386, 1750
Kurtz D. W., Martinez P., Koen C., Sullivan D. J., 1996, MNRAS, 281, 883
Kurtz D. W., Shibahashi H., 1986, MNRAS, 223, 557
Kurtz D. W., van Wyk F., Roberts G., Marang F., Handler G., Medupe R., Kilkenny D., 1997, MNRAS, 287, 69
Martinez P., Kurtz D. W., 1990, MNRAS, 242, 636
—, 1994, MNRAS, 271, 118
Martinez P., Kurtz D. W., Heller C. H., 1990, MNRAS, 246, 699
Matthews J. M., Kurtz D. W., Wehlau W. H., 1987, ApJ, 313, 782
Medupe R., Kurtz D. W., Elkin V. G., Mguda Z., Mathys G., 2015, MNRAS, 446, 1347
Murphy S. J., Saio H., Takada-Hidai M., Kurtz D. W., Shibahashi H., Takata M., Hey D. R., 2020, MNRAS, 498, 4272
Ofodum C. N., Okeke P. N., 2016, New Astron., 43, 42
Pecaut M. J., Mamajek E. E., 2013, ApJS, 208, 9
Reyniers K., Smeyers P., 2003, A&A, 404, 1051
Saio H., 2005, MNRAS, 360, 1022
—, 2014, in IAU Symposium, Vol. 301, Precision Asteroseismology, Guzik J. A., Chaplin W. J., Handler G., Pigulski A., eds., pp. 197–204
Samus N. N., Kazarovets E. V., Durlevich O. V., Kireeva N. N., Pastukhova E. N., 2017, Astronomy Reports, 61, 80
Skiff B. A., 2014, VizieR Online Data Catalog, 1, 2023
Smalley B., Niemczura E., Murphy S. J., et al., 2015, MNRAS, 452, 3334
Stibbs D. W. N., 1950, MNRAS, 110, 395
Xiong D. R., Deng L., Zhang C., Wang K., 2016, MNRAS, 457, 3163